https://doi.org/10.5194/egusphere-2022-1010
Preprint. Discussion started: 15 November 2022

Robust 4D Climate Optimal Flight Planning in Structured Airspace using Parallelized Simulation on GPUs: ROOST V1.0

Abolfazl Simorgh[1], Manuel Soler[1], Daniel González-Arribas[1], Florian Linke[2,3], Benjamin Lührs[2], Maximilian M. Meuser[2,3], Simone Dietmüller[4], Sigrun Matthes[4], Hiroshi Yamashita[4], Feijia Yin[5], Federica Castino[5], Volker Grewe[4,5], and Sabine Baumann[4]

[1]Department of Aerospace Engineering, Universidad Carlos III de Madrid, Madrid, Spain
[2]Hamburg University of Technology (TUHH), Hamburg, Germany
[3]Deutsches Zentrum für Luft- und Raumfahrt, Air Transportation Systems, Hamburg, Germany
[4]Deutsches Zentrum für Luft- und Raumfahrt, Institut für Physik der Atmosphäre, Oberpfaffenhofen, Germany
[5]Faculty of Aerospace Engineering, Delft University of Technology, Delft, The Netherlands

Correspondence: A. Simorgh (abolfazl.simorgh@uc3m.es)

Abstract. The climate impact of the non-CO_2 emissions, being responsible for two-thirds of aviation radiative forcing, highly depends on the atmospheric chemistry and weather conditions. Hence, by planning aircraft trajectories to reroute areas where the non-CO_2 climate impacts are strongly enhanced, called climate-sensitive regions, there is a potential to reduce aviation-induced non-CO_2 climate effects. Weather forecast is inevitably uncertain, which can lead to unreliable determination of climate-sensitive regions and aircraft dynamical behavior and, consequently, inefficient trajectories. In this study, we propose robust climate optimal aircraft trajectory planning within the currently structured airspace considering uncertainties in the standard weather forecasts. The ensemble prediction system is employed to characterize uncertainty in the weather forecast, and climate-sensitive regions are quantified using the prototype algorithmic climate change functions. As the optimization problem is constrained by the structure of airspace, it is associated with hybrid decision spaces. To account for discrete and continuous decision variables in an integrated and more efficient manner, the optimization is conducted on the space of probability distributions defined over flight plans instead of directly searching for the optimal profile. A heuristic algorithm based on the augmented random search is employed and implemented on graphics processing units to solve the proposed stochastic optimization computationally fast. An open-source Python library called ROOST (V1.0) is developed based on the aircraft trajectory optimization technique. The effectiveness of our proposed strategy to plan robust climate optimal trajectories within the structured airspace is analyzed through two scenarios: a scenario with large contrails' climate impact and a scenario with no formation of persistent contrails. It is shown that, for a night-time flight from Frankfurt to Kyiv, a 55% reduction in climate impact can be achieved at the expense of a 4% increase in the operating cost.

Keywords: Climate change; Aircraft trajectory optimization; Algorithmic climate change functions; Meteorological forecast uncertainty; Robustness; Graphics processing units; Structured airspace; ROOST.

https://doi.org/10.5194/egusphere-2022-1010
Preprint. Discussion started: 15 November 2022

1 Introduction

The aviation industry has experienced strong growth in recent years (Lee et al., 2021). The air traffic is estimated to grow at a 4.3% annual rate over the next 20 years (Scherer, 2019). Aviation's contribution to global warming through CO_2 and non-CO_2 emissions is currently responsible for 3.5% of total anthropogenic radiative forcing (RF) (Lee et al., 2021). The non-CO_2 climate impact includes nitrogen oxides (NO_x) induced changes in ozone and methane concentrations, water vapor (H_2O), hydrocarbons (HC), carbon monoxide (CO), sulfur oxides (SO_x), and increased cloudiness due to persistent contrail formation. Accounting for the growth rate of air traffic, a critical increase in its associated climate impact is foreseen.

Mitigating the climate impact associated with aviation-induced CO_2 emissions requires progressing along with technical aspects, such as moving toward more efficient aircraft and using novel propulsion as well as sustainable aviation fuel. Technological improvements can only be moderately inaugurated into the existing aircraft fleet. This is due to the aircraft's long life service and long phases in development, production, and certification. On the other hand, the climate impact caused by non-CO_2 emissions, contributing approximately two times higher than CO_2 emissions to aviation's global warming (Lee et al., 2021), reveals a high spatial and temporal dependency (Grewe et al., 2014b). Such dependencies provide the possibility to mitigate their climate effects through operational strategies, particularly aircraft trajectory optimization to avoid areas sensitive to aircraft emissions, called climate-sensitive regions (e.g. Simorgh et al., 2022).

Numerous studies have been proposed to reduce the climate impacts of non-CO_2 emissions through changing aircraft maneuvers to avoid climate-sensitive regions. These studies differ mainly in 1) how the climate-sensitive areas are defined and 2) how climate-friendly trajectories are determined. The first attempts to consider 'climate hotspots' were based on areas sensitive to the formation of persistent contrails (see Gierens et al. (2008)). In order to provide information on the spatial and temporal dependency of non-CO_2 effects, climate change functions (CCFs) were developed. These CCFs provide the climate impact of aviation emissions per flown kilometer and per emitted mass of the species as five-dimensional data sets (i.e., longitude, latitude, altitude, time, type of emission) (Matthes et al., 2012; Frömming et al., 2013; Grewe et al., 2014b). Due to their computational complexity, CCFs were unsuitable for real-time operations. Therefore, the so-called algorithmic climate change functions (aCCFs) were developed. The aCCFs provide a very fast computation of the individual non-CO_2 climate impact, as they are based on mathematical formulas which only need relevant local meteorological input parameters (e.g., van Manen and Grewe, 2019). The aCCFs are well-suited for trajectory optimization tools due to their computational efficiency (Matthes et al., 2017). An enhanced and consistent set (with respect to emission scenario, metrics, etc.) of aCCFs (aCCF-V1.1) have been recently developed and introduced within the EU project FlyATM4E (see Yin et al. (2022); Dietmüller et al. (2022); Matthes et al. (2022)).

As for climate optimal trajectory planning methods, various strategies ranging from mathematical programming (e.g., Campbell et al. (2008)) to meta-heuristic (e.g., Yin et al. (2018a); Yamashita et al. (2020)), indirect optimal control (e.g., Sridhar et al. (2011)), and direct optimal control methods (e.g., Niklaß et al. (2017); Lührs et al. (2021, 2016); Matthes et al. (2020)) have been adopted. For instance, the direct optimal control approach has been employed by Hartjes et al. (2016) to minimize flight time (or distance flown) in areas sensitive to persistent contrail formation, by Lührs et al. (2021) to minimize average

https://doi.org/10.5194/egusphere-2022-1010
Preprint. Discussion started: 15 November 2022

temperature response over the next 20 years (ATR20) associated with the non-CO_2 emissions, and by Vitali et al. (2021) to minimize the global warming potential (GWP) of NO_x, H_2O, soot, SO_2, and contrails. Using aCCFs to quantify climate impacts, Yamashita et al. employed a genetic algorithm to determine climate optimal aircraft trajectories (Yamashita et al., 2020, 2021). A classification of the most recent studies in this field is provided in Table 1. Interested readers are referred to Simorgh et al. (2022) for our recent, comprehensive survey on climate optimal aircraft trajectory planning, reviewing both the approaches to model climate-sensitive regions and trajectory planning methods.

To quantify the non-CO_2 climate effects, some weather variables are required. In the case of aCCFs, variables such as temperature (T), potential vorticity (PV), geopotential (Φ), relative humidity over ice (r_{hum}), and outgoing longwave radiation (OLR) are needed. These variables can be obtained from standard weather forecasts. Several factors, including incomplete understanding of the state of the atmosphere, computational complexity, and nonlinear and sometimes chaotic dynamics, affect the accuracy of weather predictions, implying that the weather forecast is inevitably uncertain (WMO, 2012). These weather forecast-related uncertainties in the aCCFs and also in aircraft dynamical behavior (e.g., uncertainty in wind and temperature), if not accounted for within aircraft trajectory planning, can lead to inefficient trajectories. Studies in the field of climate optimal aircraft trajectory planning have been performed in a deterministic manner without taking into account any sources of uncertainty (see Table 1) (Simorgh et al., 2022). A first step in managing and integrating meteorological uncertainties into aircraft path planning is to obtain reliable weather forecasts that can predict probable variations in meteorological conditions. To characterize weather forecast uncertainties, probabilistic weather forecasting (PWF) is typically used (AMS-Council, 2008). State-of-the-art probabilistic weather forecasting is obtained from the ensemble prediction system (EPS), which provides N_{EPS} possible realizations of meteorological conditions called ensemble members (Bauer et al., 2015).

When accounting for the ensemble weather forecast in solving aircraft trajectory optimization, the computational time is an important issue that arises besides the capability to consider such uncertainties. This is due to the fact that, instead of taking one weather forecast and solving the trajectory optimization in a deterministic manner, the optimizer should be capable of considering N_{EPS} (e.g., N_{EPS} = 50) different forecasts. Several studies have been proposed in the literature to determine robust aircraft trajectories in the presence of meteorological uncertainty quantified using EPS weather forecast (though not considering climate impact (Simorgh et al., 2022)). However, these studies suffer mainly from computational perspectives and some restrictive assumptions (see Simorgh et al. (2022), Subsection 5.3). In this respect, developing efficient trajectory optimization solvers capable of delivering robust climate optimal trajectories with the computational time compatible with operations has been identified as a scientific gap (see Simorgh et al. (2022)).

The focus of recent studies has been restricted to planning climate optimal trajectories considering the concept of future free-route airspace (see last column Table 1); thus, not applicable for the structured airspace of today. The trajectory optimization problem constrained by the structure of airspace results in hybrid decision spaces (e.g., route and flight level are discrete, and speed schedule is continuous) (Gonzalez Arribas et al., 2020). The trajectory optimization problem with the combination of discrete and continuous decision variables is one of the most challenging optimization problems, typically solved using mixed-integer nonlinear programming with intensive computational cost (e.g., see Bonami et al. (2013)).

https://doi.org/10.5194/egusphere-2022-1010
Preprint. Discussion started: 15 November 2022

Table 1. A classification of the recent studies in the literature proposed to reduce the climate impact of aircraft emissions with aircraft trajectory optimization.

Source	*Climate variable*	*Optimization method*	*Type*	*Routing*
Soler et al. (2014)	CO_2, Contrails	Multiphase mixed-integer optimal control	Deterministic	Free-routing
Grewe et al. (2014a)	NO_x, H_2O, CO_2, Contrails	Brute force algorithm	Deterministic	North atlantic track system
Hartjes et al. (2016)	Contrails	Direct optimal control	Deterministic	Free-routing
Lührs et al. (2016)	NO_x, H_2O, CO_2, Contrails	Direct optimal control	Deterministic	Free-routing
Lim et al. (2017)	Contrails, CO_2	Nonlinear programming	Deterministic	Free-routing
Matthes et al. (2017)	NO_x, H_2O, CO_2, Contrails	Direct optimal control	Deterministic	Free-routing
Niklaß et al. (2017)	NO_x, H_2O, CO_2, Contrails	Direct optimal control	Deterministic	Free-routing
Yin et al. (2018b)	Ozone	Genetic algorithm	Deterministic	Free-routing
Yin et al. (2018a)	Contrails	Genetic algorithm	Deterministic	Free-routing
Niklaß et al. (2019)	NO_x, H_2O, CO_2, Contrails	Direct optimal control	Deterministic	Free-routing
Yin et al. (2022)	NO_x, H_2O, CO_2, Contrails	Genetic algorithm	Deterministic	Free-routing
Yamashita et al. (2020)	NO_x, H_2O, CO_2, Contrails	Genetic algorithm	Deterministic	Free-routing
Matthes et al. (2020)	NO_x, H_2O, CO_2, Contrails	Direct optimal control	Deterministic	Free-routing
Lührs et al. (2021)	NO_x, H_2O, CO_2, Contrails	Direct optimal control	Deterministic	Free-routing
Yamashita et al. (2021)	NO_x, H_2O, CO_2, Contrails	Genetic algorithm	Deterministic	Free-routing

Drawing upon the brief literature review and the presented open problems, we aim to address the problem of determining robust climate optimal aircraft trajectory within the structured airspace in this study. Our main contributions are summarized as follows: 1) full 4D climate optimal trajectory planning within the currently structured airspace, 2) accounting for uncertain meteorological conditions and uncertainty associated with initial flight conditions such as departure time and aircraft initial mass, and 3) determining the optimized trajectory computationally very fast. The uncertainty in weather forecast is characterized using the ensemble prediction system, and aviation's climate impacts are quantified by employing the latest version of aCCFs (V1.1). The concept of robustness that we refer to is the determination of the aircraft trajectory considering all possible realizations of meteorological variables provided using an EPS weather forecast. In other words, instead of planning a trajectory based on one forecast in a deterministic manner, we aim to determine a trajectory that is optimal considering the overall performance obtained from using different members of an ensemble weather forecast. In this respect, from the operational point of view, the optimized trajectory is tracked as determined, and the effects of meteorological uncertainties are reflected

https://doi.org/10.5194/egusphere-2022-1010
Preprint. Discussion started: 15 November 2022

in the flight performance variables such as flight time, fuel burn, and climate impact. Mathematically, the perturbations due to the meteorological uncertainty are considered in the dynamical model of aircraft, and the proposed trajectory optimization is generic in terms of the objective function, in which a wide range of objectives, such as flight time, fuel consumption, emissions, and climate impact, and different statistics including expected values and variance of the performance variables can be considered. Such flexibility in defining the cost function allows for solving a multi-objective optimization problem. Moreover, by penalizing the mean and variance of the objectives, the effects of uncertainty on flight variables can be controlled. In this study, the flight planning objective is a weighted sum of the simple operating cost (as a function of flight time and fuel consumption) and climate impact, and the focus is restricted to the optimization of the expected performance since, as it will be shown in the simulation results, for the considered case studies, the minimization of the averaged performance leads to reducing the uncertainty ranges.

We employ the probabilistic flight planning method firstly developed by Gonzalez Arribas et al. (2020) to determine robust climate optimal trajectories for three phases: climb, cruise, and descent. In this approach, to account for discrete and continuous decision variables in an integrated manner, the optimization is carried out on the space of probability distributions defined over flight plans instead of directly searching for the optimal profile. Then, the probability distribution over flight plans is parameterized, allowing to generate multiple flight plans stochastically. The augmented random search algorithm is employed and implemented on GPUs to deliver a near-optimal solution to the resulting stochastic optimization in seconds. We have developed an open-source Python library called ROOST V1.0 (Robust Optimization of Structured Trajectories) based on the proposed robust aircraft trajectory optimization technique, which is currently available via DOI (https://doi.org/10.5281/zenodo.7121862). ROOST is a tool that efficiently uses the information provided by the prototype aCCFs (implemented in our recently developed python library CLIMaCCF V1.0 (DOI: https://doi.org/10.5281/zenodo.6977273) (Dietmüller et al., 2022)) for planning climate optimal trajectories accounting for the operational constraints and uncertainty. Users need to input the required weather variables, route graphs, and aircraft type specifications to start working with the library. In addition, users should assign values to the weighting parameters associated with different objectives in the objective functions. This paper is mainly devoted to the climate optimal aircraft trajectory planning algorithm implemented in the library and its application to optimize different case studies. Instructions to get started with the library can be found in the repository of ROOST.

The manuscript is arranged as follows. The robust climate optimal aircraft trajectory planning problem is presented and solved in Section 2. The potential of our flight planning algorithm in reducing aviation's climate impacts under uncertain meteorological conditions is explored in Section 3. The discussion on the obtained results is performed in Section 4, and some concluding remarks close the paper in Section 5.

2 Robust climate optimal aircraft flight planning

The robust aircraft trajectory optimization problem within the structured airspace accounting for climate impacts is stated, formulated, and solved in this section. Subsection 2.1 presents the deterministic climate optimal aircraft trajectory planning problem. In Subsection 2.2, the effects of uncertainty on the efficiency of the planned climate optimal trajectory are discussed,

https://doi.org/10.5194/egusphere-2022-1010
Preprint. Discussion started: 15 November 2022

and the motivation to solve robust trajectory optimization is provided. Then, the trajectory optimization problem (stated in Subsection 2.1) is reformulated in Subsection 2.3 to account for uncertainties. Finally, the approach to solving the robust trajectory optimization problem is presented in Subsection 2.4.

2.1 Deterministic climate optimal aircraft flight planning: optimal control problem formulation

Let us consider a dynamical system with the state-space representation as: $\dot{\mathbf{x}}$(t)=f$\big($t,z, x(t),u(t)$\big)$, where $\mathbf{u} \in \mathbb{R}^{n_u}$, $\mathbf{x} \in \mathbb{R}^{n_x}$, and $\mathbf{z} \in \mathbb{R}^{n_z}$ are the vectors of control inputs, states and algebraic variables, respectively and $\mathbf{f}$ is a vector field, mapping $\mathbb{R} \times \mathbb{R}^{n_z} \times \mathbb{R}^{n_x} \times \mathbb{R}^{n_u} \rightarrow \mathbb{R}^{n_x}$. A general formulation of the optimal control can be stated as follows:

$$\min_{u \in \mathcal{U}} J(t_0, t_f, \mathbf{x}, \mathbf{u}) = \mathcal{M}\big(t_0, t_f, \mathbf{x}(t_0), \mathbf{x}(t_f)\big) + \int_{t_0}^{t_f} \mathcal{L}\big(t, \mathbf{x}(t), \mathbf{u}(t), \mathbf{z}\big) \mathrm{d}t \tag{1}$$

with respect to :
$$\dot{\mathbf{x}}(t) = \mathbf{f}\big(t, \mathbf{z}, \mathbf{x}(t), \mathbf{u}(t)\big) \tag{2}$$
$$\mathbf{h}\big(\mathbf{x}(t), \mathbf{u}(t), \mathbf{z}\big) = \mathbf{0} \tag{3}$$
$$\mathbf{g}\big(\mathbf{x}(t), \mathbf{u}(t), \mathbf{z}\big) \leq \mathbf{0} \tag{4}$$
$$\Psi\big(t_0, t_f, \mathbf{x}(t_0), \mathbf{x}(t_f)\big) = \mathbf{0} \tag{5}$$

where Eq. (1) is the objective function including mathematically interpreted goals of optimization with $M : \mathbb{R} \times \mathbb{R} \times \mathbb{R}^{n_x} \times \mathbb{R}^{n_x} \rightarrow \mathbb{R}$ and $L : \mathbb{R} \times \mathbb{R}^{n_x} \times \mathbb{R}^{n_u} \times \mathbb{R}^{n_z} \rightarrow \mathbb{R}$ as the Mayer and Lagrange terms called terminal cost and cost-to-go, respectively. The objective is to find a feasible control policy ($u \in \mathcal{U}$) to minimize the performance index (Eq. (1)) respecting a set of constraints, including dynamical constraints (Eq. (2)), equality and inequality path constraints (Eqs. (3,4)), and boundary constraints (Eq. (5)). Notice that the optimal control problem stated here is a general form. Depending on the benchmark problem, reformulations and approximations are normally made to address the required performance, such as computational complexity. For instance, within the current formulation, the decision variable is only the control policy in the continuous domain; however, within some numerical approaches, such as the direct collocation approach, the system's states are also considered as decision variables and represented in a discrete fashion. In this study, we will slightly reformulate the optimal control problem for the proposed path planning problem.

The definition of trajectory optimization problem within the context of optimal control theory mainly requires the aircraft dynamical model, objective function, and physical and operational constraints. To consider climate impact within aircraft trajectory planning, information on the climate impacts of CO_2 and non-CO_2 emissions ~~is~~ necessary and needs to be included in the objective function. In the following, the modeling of the mentioned elements is briefly presented.

2.1.1 Aircraft dynamical model

To determine reliable aircraft trajectories, accurate aircraft dynamical models are necessary. In this work, the point-mass model with the following equations of motion is used to represent the aircraft's dynamical behavior, as is usually considered within

https://doi.org/10.5194/egusphere-2022-1010
Preprint. Discussion started: 15 November 2022

air traffic management studies

$$\begin{bmatrix} \dot{\phi} \\ \dot{\lambda} \\ \dot{h} \\ \dot{v} \\ \dot{m} \end{bmatrix} = \begin{bmatrix} \big(v\cos\gamma\cos\chi + w_y\big)\big(R_M(\phi)+h\big)^{-1} \\ \big(v\cos\gamma\sin\chi + w_x\big)\big((R_N(\phi)+h)\cos\phi\big)^{-1} \\ v\sin\gamma \\ \big(T(C_T) - D(C_L)\big)m^{-1} - g\sin\gamma \\ -FF(C_T) \end{bmatrix},$$

$$\text{State variables } (\mathbf{x}): \begin{bmatrix} \phi & \lambda & h & v & m \end{bmatrix}^T,$$

$$\text{Control variables } (\mathbf{u}): \begin{bmatrix} C_T & \chi & \gamma \end{bmatrix}^T. \tag{6}$$

where ϕ is the latitude, λ is the longitude, v is the true airspeed, h is the altitude, m is the mass, C_T is the thrust coefficient, γ is the climb angle, χ is the heading angle, $C_L(\gamma) = (2mg\cos\gamma)/(\rho v^2 S)$, and (w_x, w_y) are wind~~'s~~ components. The Earth's ellipsoid radii of curvature in the meridian and the prime vertical are denoted with R_M and R_N, respectively, T is the magnitude thrust force and the drag force is denoted with D. g is the Earth's gravity, FF is the fuel flow and S is the wetted surface of the aircraft. BADA model (Gallo et al., 2006) is employed to provide the aerodynamic and propulsive performance of the aircraft.

Structured airspace

As trajectory optimization in this study is performed within the structured airspace, the evolutions of aircraft~~'s~~ states are constrained. In the following, we briefly present our proposed modeling of airspace structure and flight plan.

We consider a directed acyclic graph $G = (V, E)$ to model the airspace with V as the navigation waypoints and $e \in E$ as the airway edges connecting waypoints. The trajectory is assumed to start at the end of the standard instrument departure procedure (SID) and end at the beginning of the standard instrument arrival procedure (STAR) to the destination airport, denoted as $o \in V$ and $d \in V$, respectively. We define the flight plan F with a tuple $(R, \overline{\text{FL}}, \overline{\text{M}}, C, D, d_D)$. In the flight plan (F), the route (or lateral path) denoted as R includes a sequence of waypoints i.e., $R := (r_0, r_1, \cdot, r_{n_r})$. The vertical profile of the cruise, $\overline{\text{FL}}$, is composed of an ordered sequence of tuples of the form (r_k, FL_k), indicating that, if the aircraft is in the cruise phase, the flight level will be changed to FL_k when the waypoint r_k is reached (see Fig. 1). The Mach schedule $\overline{\text{M}} := (\text{M}_0, \cdots, \text{M}_{n_r})$ indicates the target Mach number M_k at waypoint r_k, during the cruise phase. Climb and descent profiles $C, D : \mathbb{R} \to \mathbb{R}$ are represented by continuous and piecewise-differentiable functions mapping the altitude to the target airspeed during the climb and descent phases, respectively. Finally, a scalar variable d_D shows the distance-to-go to the destination node at which the aircraft should end the cruise and start the descent phase.

https://doi.org/10.5194/egusphere-2022-1010
Preprint. Discussion started: 15 November 2022

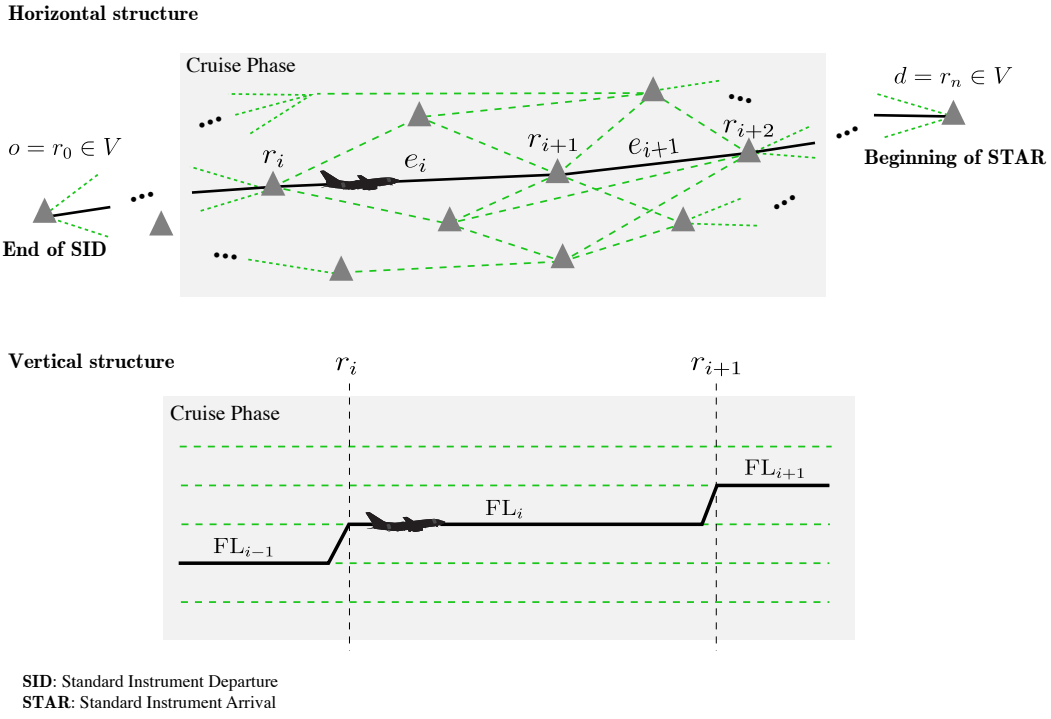

Figure 1. Structure of airspace. The route graph is generated by processing the full airspace graph to include paths from the end of the SID to the beginning of the STAR to the destination airport.

2.1.2 Objective function

The goals of the aircraft trajectory optimization problem are interpreted mathematically and defined as an objective function to be minimized (or maximized). In addition to the climate impact, the operating cost is a crucial aspect that needs to be considered as it is one of the main interests of airliners. Generally, there is a trade-off between the operating cost and climate impacts. This is due to the fact that rerouting sensitive areas to climate increases the operational costs as the aircraft tends to fly longer routes (Niklaß et al., 2021). To consider both objectives in the trajectory optimization, we define the following objective function:

$$\text{Objective function} = \psi_{\text{CST}} \cdot \text{Operating cost} + \psi_{\text{CLM}} \cdot \text{Climate impact} \tag{7}$$

where ψ_{CST} and ψ_{CLM} are weighting parameters penalizing cost and climate impact, respectively. In the following, the proposed modeling of these two objectives is presented.

https://doi.org/10.5194/egusphere-2022-1010
Preprint. Discussion started: 15 November 2022

Operating cost

There exist various approaches to account for operating costs within aircraft path planning. Flight time or/and fuel are common objectives. However, more realistic cost metrics exist, which include additional costs such as flight crew, cabin crew, and landing fees. Interested readers are referred to Simorgh et al. (2022) for a classification of these metrics.

In this study, we use simple operating cost (SOC) as a metric expressing cost in USD with linear relation to flight time and fuel consumption:

$$\text{Operating cost} = \psi_t \cdot (t_f - t_0) + \psi_m \cdot (m_0 - m_f) \tag{8}$$

where t_0 and t_f are the initial flight time and final flight time weighted by ψ_t = 0.75 [USD/s], and m_0 and m_f are the initial mass and final mass weighted by ψ_m = 0.51 [USD/kg]. In spite of considering only flight time and fuel burn to represent the operating cost, it was reported in Table 4 of Yamashita et al. (2021) that employing SOC and a more comprehensive metric such as cash operating cost within trajectory optimization delivered almost similar results. This is mainly related to the consideration of time and fuel burn to calculate costs of other aspects such as crew's salaries.

Climate impact

Numerous approaches have been proposed in the literature to consider climate impact within aircraft trajectory planning strategies (see Table 1 and Figure 2 of (Simorgh et al., 2022)). In this study, the climate impact of aircraft operations is modeled using the prototype aCCFs. The suitability of aCCFs for climate optimal trajectory planning can be justified as follows:

- aCCFs account for the temporal and spatial dependency of climate impacts associated with non-CO_2 species, including ozone and methane, resulted from NO_x emissions, water vapor emissions, and persistent contrails.
- aCCFs estimate the climate impact associated with aircraft emissions computationally in real-time, making it well-suited for climate optimal trajectory planning.
- aCCFs directly quantify climate impacts in average temperature change.

In this study, we adopt aCCF-V1.1 developed by Matthes et al. (2022) within the EU project FlyATM4E. The aCCF-V1.1 is based on aCCF-V1.0 but includes educated guess factors to address the uncertainty associated with the current level of scientific understanding of aviation's climate impact effects. The aCCF-V1.0 reported by Yin et al. (2022) (which is the basis for developing the aCCF-V1.1), is the first complete and consistent set of prototype aCCFs, providing spatial and temporal dependent non-CO_2 climate effects in terms of average temperature response over the next 20 years for pulse emission scenario (P-ATR20).

The suitability of the physical climate metrics is application-dependent (Grewe and Dahlmann, 2015). As for mitigating the climate impacts of aviation with trajectory planning, average temperature response over the next 20 years with business-as-usual (BAU) future emission scenario is a suitable choice (Grewe et al., 2021). To this end, the aCCFs based on the pulse emission scenario are converted to the future scenario (F-ATR20) using values reported in Table 3 of Dietmüller et al. (2022).

https://doi.org/10.5194/egusphere-2022-1010
Preprint. Discussion started: 15 November 2022

The aCCFs are further scaled by using efficacy parameters reported by Dietmüller et al. (2022) to account for the effectiveness of non-CO_2 forcing agents in changing global mean temperature compared to that of CO_2 (see Dietmüller et al. (2022) for a detailed description). For the sake of compactness of notation, F-ATR20 with educated guess factors and efficacy parameters is replaced with ATR in the following.

For the aCCFs of (day-time and nigh-time) contrails, the ice-supersaturation is applied, using temperature and relative humidity over ice in order to predict regions where persistent contrails are expected to form, called persistent contrails formation areas (PCFA) (Schmidt, 1941; Appleman, 1953). To represent the climate impacts using aCCFs in the average temperature change (i.e., [K]), fuel consumption rate, NO_x emission, and distance flown through PCFA are required.

The geographical aCCF pattern of water vapour, NO_x induced ozone and methane, as well as of contrail is shown in Fig. 2a-c for 13th of June 2018, 00:00 UTC over the European region at pressure level 250hPa. Moreover, Fig. 2d shows the pattern of the merged non-CO_2 aCCFs that combines the individual aCCFs (Fig. 2a-c). Note that to generate the merged aCCFs and to compare the contribution of each species, we adopt typical transatlantic fleet mean values to unify the units of aCCFs in K/kg(fuel). The approximated conversion factors for NO_x emission and contrails are 13×10^{-3}Kg(NO_2)/Kg(fuel) and $0.16 \times$ km/Kg(Fuel), respectively (Graver and Rutherford (2018), Penner et al. (1999)). It is clear from the merged aCCFs that the contrails have dominant climate effects, which is in line with related studies employing aCCFs (e.g., see Dietmüller et al. (2022)).

To benefit from the spatial and temporal dependency of non-CO_2 climate effects identified using aCCFs in planning climate optimal trajectories, we define the following objective expressed in Lagrange form for Eq. (7):

$$\text{Climate impact} = \int_{t_0}^{t_f} \sum_{i=1}^{5} \psi_{\text{ATR},i} \cdot \text{ATR}_i\big(t, \mathbf{x}(t), \mathbf{u}(t)\big)\,\mathrm{d}t \tag{9}$$

for $i \in \{\text{CH}_4, \text{Cont.}, \text{O}_3, \text{H}_2\text{O}, \text{CO}_2\}$:

$$\begin{aligned}
&\text{ATR}_{\text{O}_3}(t,\mathbf{x},\mathbf{u}) = 10^{-3} \times \text{aCCF}_{\text{O}_3}\big(t,\mathbf{x}\big) \cdot \dot{m}_{nox}(t)\\
&\text{ATR}_{\text{CH}_4}(t,\mathbf{x},\mathbf{u}) = 10^{-3} \times \text{aCCF}_{\text{CH}_4}\big(t,\mathbf{x}\big) \cdot \dot{m}_{nox}(t)\\
&\text{ATR}_{\text{Cont.}}(t,\mathbf{x},\mathbf{u}) = 10^{-3} \times \text{aCCF}_{\text{Cont.}}(t,\mathbf{x}) \cdot v_{gs}(t)\\
&\text{ATR}_{\text{H}_2\text{O}}(t,\mathbf{x},\mathbf{u}) = -\text{aCCF}_{\text{H}_2\text{O}}(t,\mathbf{x}) \cdot \dot{m}(t)\\
&\text{ATR}_{\text{CO}_2}(t,\mathbf{x},\mathbf{u}) = -\text{aCCF}_{\text{CO}_2} \cdot \dot{m}(t)
\end{aligned} \tag{10}$$

where $\dot{m}_{nox}(t) = FF(t,\mathbf{u}) \cdot \text{EI}_{\text{NO}_x}(t,\mathbf{x},\mathbf{u})$, $\text{EI}_{\text{NO}_x}(\cdot)$ is the actual NO_x emission index in [g(NO_2)/kg(fuel)], and v_{gs} is the ground speed. The NO_x emission index varies with many factors such as aircraft type, fuel flow, flight altitude, and synoptical situation. To consider such dependencies, the Boeing fuel flow method 2 (BFFM2), calculating the actual emission index of NO_x from the reference conditions, is adopted (DuBois and Paynter, 2006; Jelinek, 2004). The reference conditions are obtained from the International Civil Aviation Organization (ICAO) data bank. Notice that the objective regarding climate impact is expressed in Lagrange (i.e., as integral) since the climate impact needs to be evaluated (and accumulated) along the route, unlike the operating cost, which requires only information on boundary values (e.g., initial and final flight time).

https://doi.org/10.5194/egusphere-2022-1010
Preprint. Discussion started: 15 November 2022

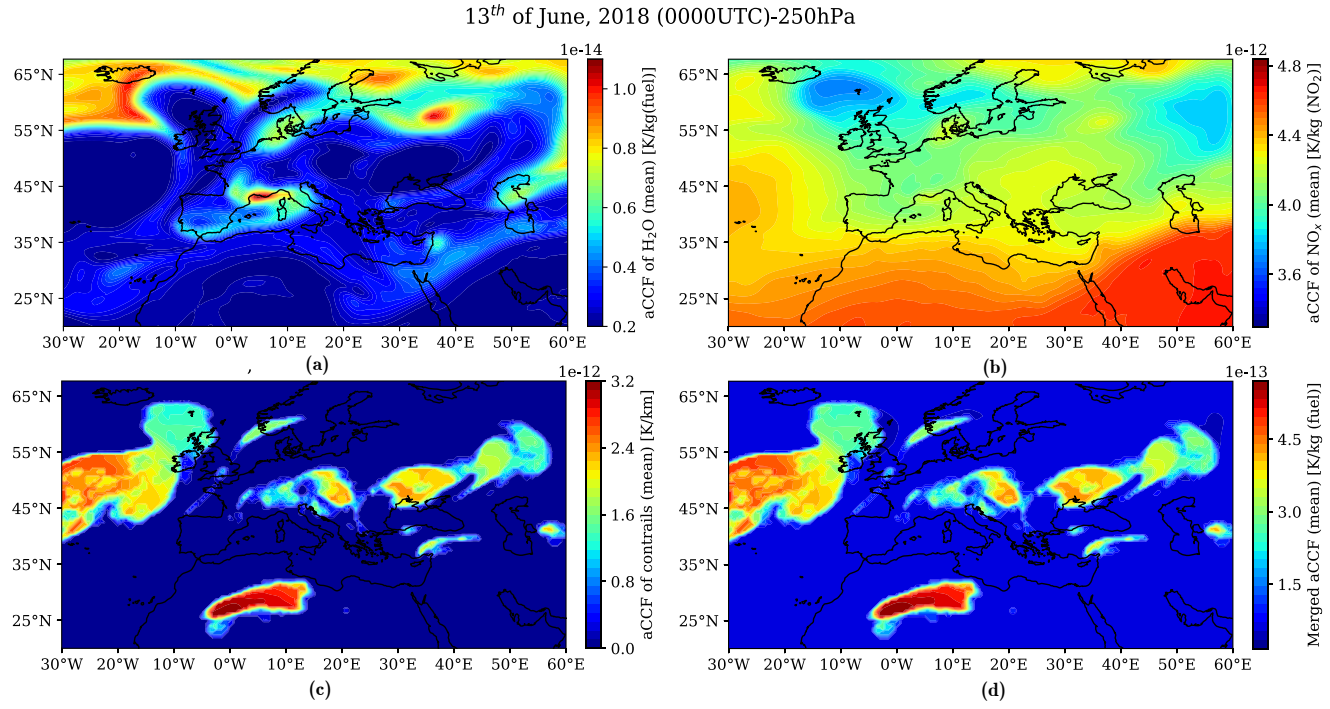

Figure 2. Algorithmic climate change functions of (a) water vapour, (b) NO_x, (c) contrails, and (d) of the total non-CO_2 effects on 13th of June 2018, 00:00 UTC over European airspace at pressure level 250hPa.

2.2 Uncertainty from weather forecast

The aircraft trajectory optimization problem within the context of optimal control theory (as formulated in Subsection 2.1) requires the aircraft dynamical model, flight objectives, and physical and operational limitations (Simorgh et al., 2022).

The dynamical model of aircraft requires weather-related variables such as wind and temperature (e.g., see Subsection 2.1.1). In addition, the non-CO_2 climate effects of aviation included in the objective function of the optimization problem strongly rely on weather conditions (see Subsection 2.1.2 in case of using aCCFs). Since the required meteorological variables are obtained from standard weather forecasts, they are inevitably uncertain. It is worth mentioning that there exist other sources of uncertainty affecting the efficiency of the planned climate optimized trajectories, including uncertainty from climate science (e.g., modeling and estimating aviation-induced climate effects), emission calculation, and also inaccurate modeling of aircraft behavior, which are not the scope of this paper but have been identified as open problems (see Matthes et al. (2022)).

In this paper, the focus is on forecast-related uncertainties, which will be characterized by employing ensemble prediction system (EPS) weather forecasts, a numerical weather prediction method introduced to deal with uncertainty in weather forecast (Bauer et al., 2015). These are forecasts in which both the initial conditions and the physical parameters of a numerical weather integration model are slightly modified from one member to another and provide N_{EPS} (typically $N_{\text{EPS}} = 50$) different predic-

https://doi.org/10.5194/egusphere-2022-1010
Preprint. Discussion started: 15 November 2022

tions known as ensemble members (Bauer et al., 2015). Each member of an ensemble represents one possible realization of meteorological situations. As the aCCFs take as inputs some meteorological variables, N_{EPS} different aCCFs can be calculated for an EPS weather forecast. For instance, meteorological variables temperature and relative humidity over ice are required for the aCCF of night-time contrails. Notice that relative humidity over ice is required for identifying ice-supersaturated areas. Feeding N_{EPS} probable realizations of these meteorological variables (i.e., ensemble members), N_{EPS} different aCCFs (i.e., $\mathrm{aCCF}_{\mathrm{Cont}_i}$ for $i = 1, \cdots, N_{\mathrm{EPS}}$) are calculated. The same applies to system dynamics (considering uncertainty in temperature and wind) and also the NO_x emission index (due to the dependency on ambient temperature and specific humidity).

To investigate the degree of uncertainty (or variability) in the meteorological variables provided by an EPS and its effects on the computed aCCFs, we take the standard deviation (STD) from ten ensemble members of weather data obtained using the ERA5 reanalysis data products[1]. It should be noted that the reanalysis data products are generated from post-processing with observations. Thus, the variability among the ensemble members is expected to be lower than the forecast data with more ensemble members, yet still is valid to illustrate. Figure 3 shows the STD of weather-variables required to calculate aCCFs and aircraft trajectory on 13$^{\mathrm{th}}$ of June 2018, 00:00 UTC, at the pressure level 250hPa. The STD is taken over the normalized variables (with respect to their maximum values) for comparison purposes. The variability of geopotential, temperature, and wind is small compared to potential vorticity, outgoing longwave radiation, and relative humidity. The STDs of the calculated aCCFs based on the ensemble members are illustrated in Fig. 4. Since the aCCF of NO_x emission (i.e., methane and ozone) depends on geopotential and temperature, its STD is small compared to the aCCFs of water vapor and night-time contrails, which are based on potential vorticity and relative humidity (when applying the ice-supersaturated condition), respectively. Notice that the uncertainty in the climate impact of contrails is much higher than water vapor due to the variability of relative humidity in satisfying the persistency condition of contrails (see STD of PCFA in Fig. 4). Due to the considered time (i.e., 00:00 UTC), the aCCF of contrails is based on the formulation of night-time aCCFs. In spite of neglectable uncertainty in the aCCF of NO_x, and also relatively low uncertainty in the aCCF of water vapor compared to aCCF of contrails, due to the dominant climate impact of contrails, the net non-CO_2 climate effect is considerably uncertain (see STD of the merged aCCFs in Fig. 4), which must be crucially taken into consideration.

Fig. 5 shows how uncertainty in meteorological variables can affect the performance of aircraft trajectories. As can be seen, these uncertainties are accumulated and can considerably degrade the efficiency of the optimized trajectory if not considered in the aircraft trajectory planning a priori. No recent study on the determination of climate-optimized trajectories has considered the robustness in the sense of uncertainty in weather forecasts. One of the main reasons for not considering such variations is the computational time that arises within the optimization techniques. In fact, instead of considering one member, the optimization, in this case, is to consider N_{EPS} ensemble members (e.g., 50) and find an optimized trajectory to be optimal with respect to all probable realizations of meteorological variables. Such an increase of dimensions is daunting to cope with employing the classical dynamical optimization approaches such as direct optimal control.

In Subsections 2.3 and 2.4, we will address the problem of robust climate optimal trajectory planning with an efficient heuristic method implemented on GPUs.

[1] https://cds.climate.copernicus.eu/

https://doi.org/10.5194/egusphere-2022-1010
Preprint. Discussion started: 15 November 2022

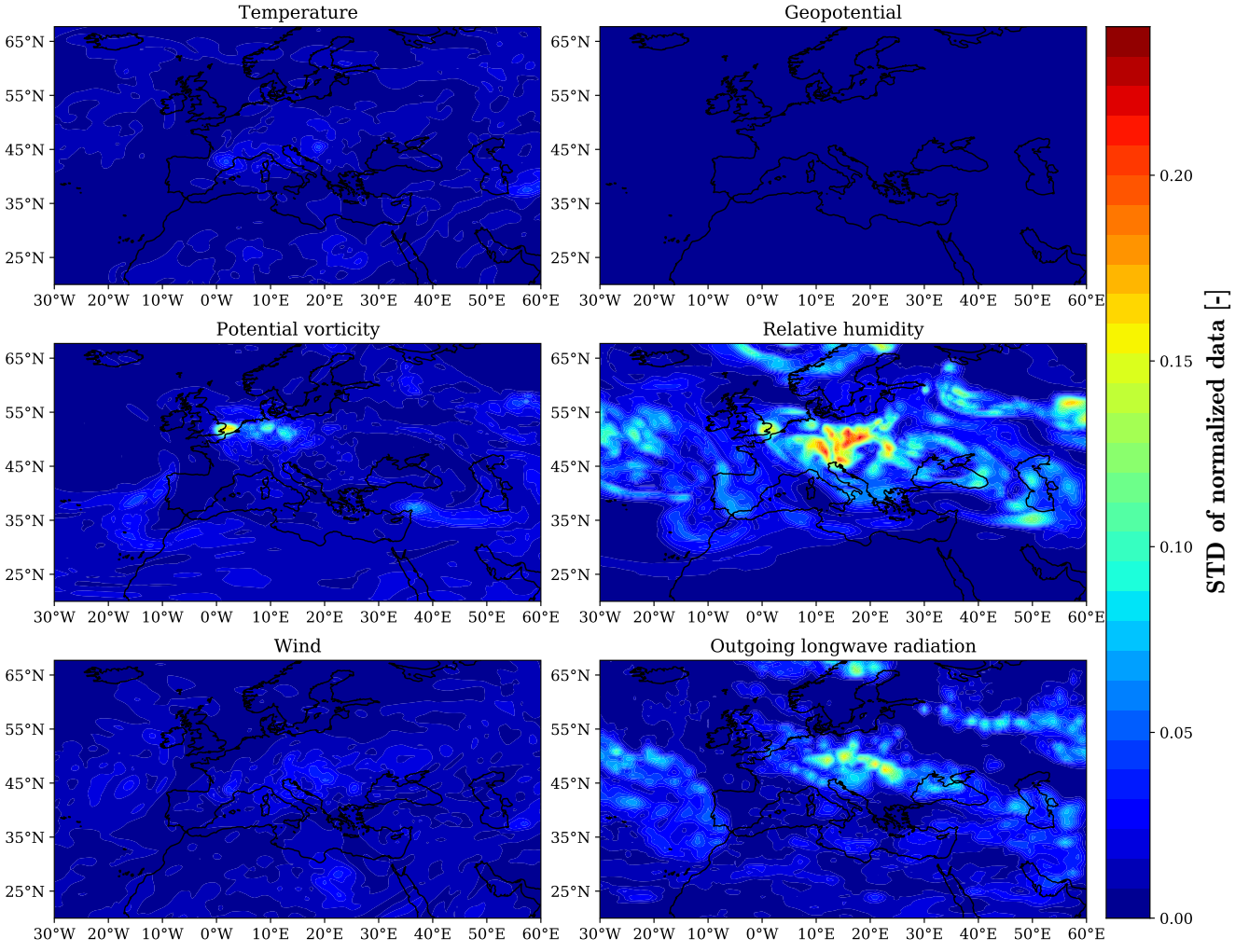

Figure 3. Variability (quantified using STD) of the meteorological conditions for an ensemble weather forecast with 10 ensemble members on 13th of June 2018, 00:00 UTC over European airspace at pressure level 250hPa.

https://doi.org/10.5194/egusphere-2022-1010
Preprint. Discussion started: 15 November 2022

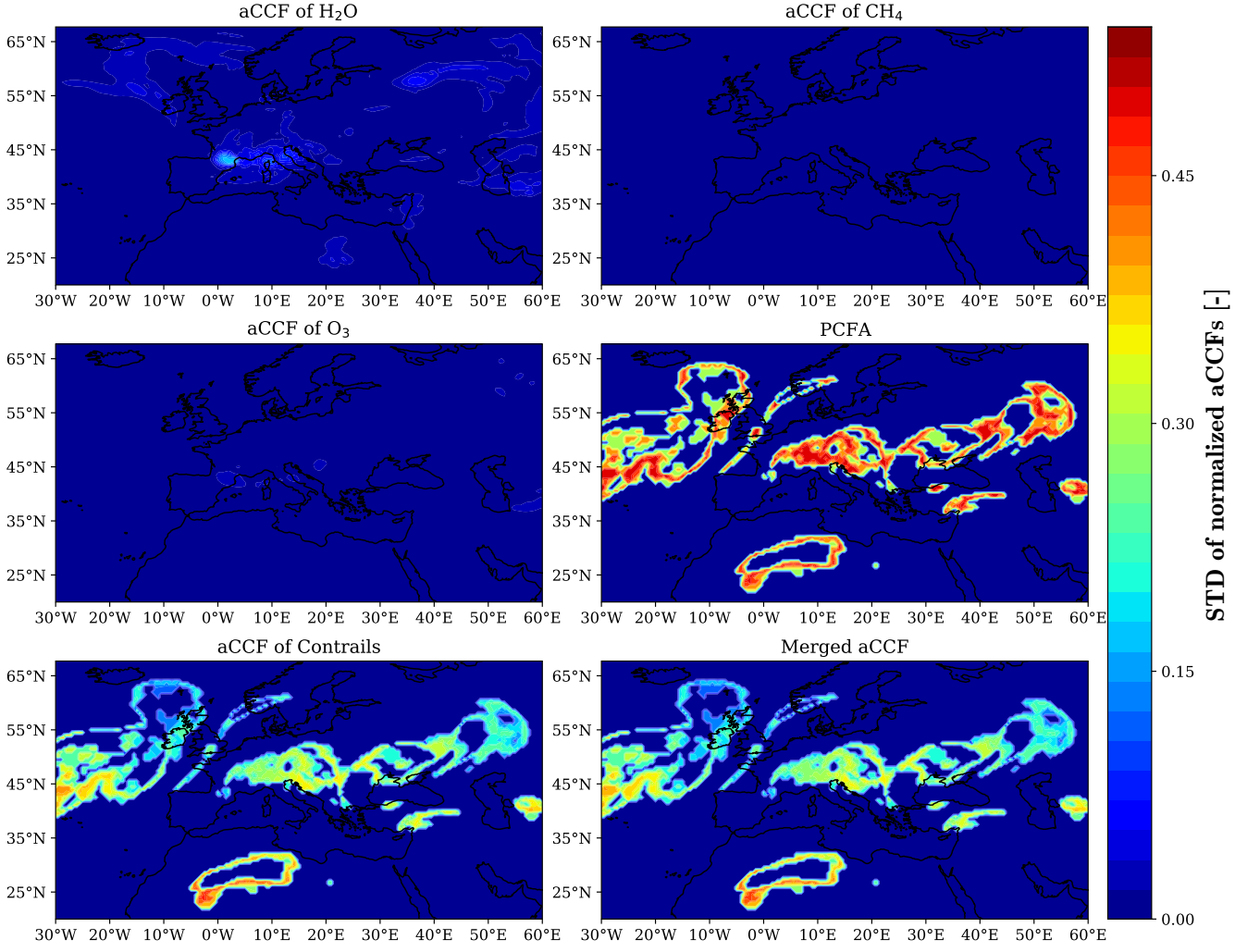

Figure 4. Variability (quantified using STD) of aCCFs for an ensemble weather forecast with 10 ensemble members on 13th of June 2018, 00:00 UTC over European airspace at pressure level 250hPa.

https://doi.org/10.5194/egusphere-2022-1010
Preprint. Discussion started: 15 November 2022

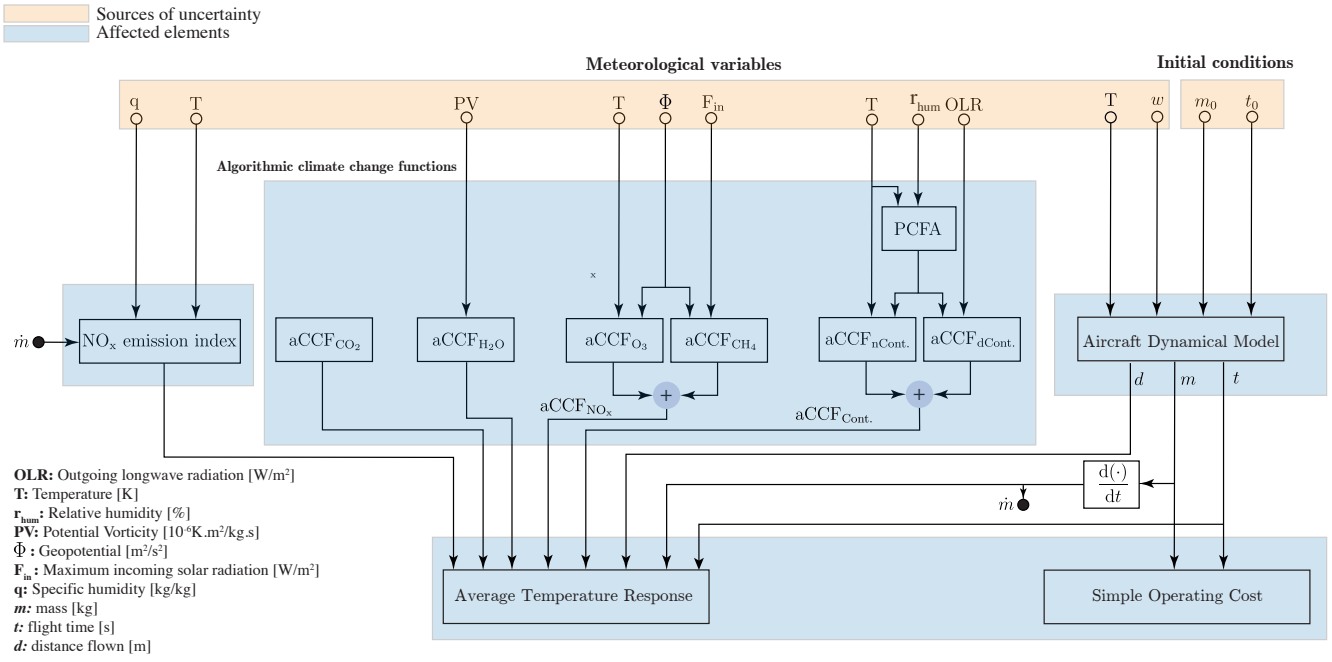

Figure 5. Propagation of uncertainties (associated with initial flight conditions and meteorological variables) within climate optimal aircraft trajectory planning.

2.3 Robust climate optimal flight planning problem formulation

In Subsection 2.1, the climate optimal trajectory planning was stated for the deterministic problem. Due to the effects of uncertainty discussed in Subsection 2.2, we redefine the optimization problem by taking into account uncertain meteorological conditions.

Let us consider a class of dynamical systems with uncertainty as follows:

$$\dot{\mathbf{x}}(t,\omega) = \mathbf{f}\big(t, \mathbf{x}(t,\omega), \mathbf{u}(t,\omega), \mathbf{z}(t,\omega), \zeta(\omega)\big). \tag{11}$$

The uncertain parameters (denoted with $\zeta \in \mathbb{R}^{n_\zeta}$) are considered as continuous random variables and assumed to have known probability distribution functions $\zeta(\cdot) : \Omega \to \mathbb{R}^{n_\zeta}$, where Ω is a space of possible outcomes. The random variables take different values depending on the probable outcomes (i.e., $\zeta(\omega)$ for $\omega \in \Omega$). The nonlinear function $\mathbf{f}(\cdot)$ is assumed to be a measurable function in ζ. To emphasise on the effects of random variables on the system's trajectories, all the variables were denoted with dependency on possible outcomes (e.g., $\mathbf{x}(t,\omega)$). For the sake of improving clarity, the abbreviated notation (e.g., $\mathbf{x}(t)$) will be used in the following. In the context of optimal control theory, the following general form of the cost functional is considered

https://doi.org/10.5194/egusphere-2022-1010
Preprint. Discussion started: 15 November 2022

for robust problems:

$$J = \mathbb{E}\Big\{ M\big(t_0, \mathbf{x}(t_0), t_f, \mathbf{x}(t_f)\big) + \int_{t_0}^{t_f} L\big(t, \mathbf{x}(t), \mathbf{u}(t), \mathbf{z}(t), \zeta\big)\mathrm{d}t \Big\} \tag{12}$$

where $M : \mathbb{R}\times\mathbb{R}^{n_x}\times\mathbb{R}\times\mathbb{R}^{n_x} \to \mathbb{R}$ and $L : \mathbb{R}\times\mathbb{R}^{n_x}\times\mathbb{R}^{n_u}\times\mathbb{R}^{n_z}\times\mathbb{R}^{n_\zeta} \to \mathbb{R}$ are the Mayer and Lagrange terms, respectively. The objective function is written in terms of using the expectation operator, however, other statistics can be evaluated under this formulation. For instance, one can include the variance of a function $A(\zeta)$ as: $\mathbb{V}\{A\} = \mathbb{E}\big\{\big(A - \mathbb{E}\{A\}\big)^2\big\} = \mathbb{E}\{A^2\} - \mathbb{E}\{A\}^2$, where $\mathbb{V}\{\cdot\}$ is the variance operator.

Within the proposed robust aircraft trajectory optimization, the uncertainty is considered in the weather forecast and initial flight conditions. To obtain a climate-optimized trajectory, we define the following performance index

$$J = \psi_{\text{CST}}\Big[\psi_t \cdot \text{ Exp. Flight time} + \psi_m \cdot \text{Exp. Fuel burnt}\Big] + \psi_{\text{CLM}} \cdot \text{Exp. ATR}$$

$$\text{Exp. Flight time} : \mathbb{E}\big\{\text{FT}\big\} := \mathbb{E}\big\{t_f - t_0\big\}$$

$$\text{Exp. Fuel burnt} : \mathbb{E}\big\{\text{FB}\big\} := \mathbb{E}\big\{m_0 - m_f\big\}$$

$$\text{Exp. ATR} : \mathbb{E}\big\{\text{ATR}\big\} := \mathbb{E}\Big\{\int_{t_0}^{t_f}\sum_{i=1}^{5}\psi_{\text{ATR},i}\cdot\text{ATR}_i\big(t, \mathbf{x}(t), \mathbf{u}(t), \zeta\big)\mathrm{d}t\Big\} \tag{13}$$

for $i \in \{\text{CH}_4, \text{Cont.}, \text{O}_3, \text{H}_2\text{O}, \text{CO}_2\}$:

$$\begin{aligned}
&\text{ATR}_{\text{O}_3}(t, \mathbf{x}, \mathbf{u}, \zeta) = 10^{-3} \times \text{aCCF}_{\text{O}_3}\big(t, \mathbf{x}, \zeta\big)\cdot\dot{m}_{nox}(t, \zeta)\\
&\text{ATR}_{\text{CH}_4}(t, \mathbf{x}, \mathbf{u}, \zeta) = 10^{-3} \times \text{aCCF}_{\text{CH}_4}\big(t, \mathbf{x}, \zeta\big)\cdot\dot{m}_{nox}(t, \zeta)\\
&\text{ATR}_{\text{Cont.}}(t, \mathbf{x}, \mathbf{u}, \zeta) = 10^{-3} \times \text{aCCF}_{\text{Cont.}}(t, \mathbf{x}, \zeta)\cdot v_{gs}(t, \zeta)\\
&\text{ATR}_{\text{H}_2\text{O}}(t, \mathbf{x}, \mathbf{u}, \zeta) = -\text{aCCF}_{\text{H}_2\text{O}}(t, \mathbf{x}, \zeta)\cdot\dot{m}(t, \zeta)\\
&\text{ATR}_{\text{CO}_2}(t, \mathbf{x}, \mathbf{u}, \zeta) = -\text{aCCF}_{\text{CO}_2}\cdot\dot{m}(t, \zeta)
\end{aligned} \tag{14}$$

which is similar to the deterministic case in the sense of objectives and formulation but associated with uncertainty. Notice that we define the objectives considering the expected performance. One can use other statistics, such as variance, without loss of generality. For instance, to penalize the range of uncertainty on climate impacts, $\mathbb{V}\{\text{ATR}\} = \mathbb{E}\{\text{ATR}^2\} - \mathbb{E}\{\text{ATR}\}^2$ should be included in the objective function. For the considered case studies, it will be shown that the minimization of the expected objective function will reduce the uncertainty on the most uncertain variable for the climate optimal routing option, thus providing a robust solution without penalizing the deviation. The forecast-related uncertainties and uncertainty associated with initial flight conditions are denoted here with the vector ζ. For instance, the uncertainty in $\text{ATR}_{\text{O}_3}(t, \mathbf{x}, \zeta)$ is due to the uncertainty in aircraft performance variables (i.e., $m(t, \zeta)$ which is affected by uncertainty in temperature and wind) and also temperature (i.e., $\text{T}(t, \mathbf{x}, \zeta)$) and geopotential (i.e., $\Phi(t, \mathbf{x}, \zeta)$) for calculating aCCF_{O_3}. For each probable realization of uncertain

https://doi.org/10.5194/egusphere-2022-1010
Preprint. Discussion started: 15 November 2022

variables $\zeta(\omega = \omega_0)$, a deterministic trajectory optimization problem can be solved. In the next section, we employ a robust optimization framework to determine climate optimal trajectories under uncertain meteorological conditions with a relatively fast algorithm.

2.4 Solution approach

The aircraft trajectory optimization problem formulated in Subsection 2.3 is solved by employing the method firstly developed by Gonzalez Arribas et al. (2020), which is a stochastic optimization technique for the structured airspace and is capable of determining the optimized trajectory in four dimensions, i.e., latitude, longitude, altitude, and time.

As mentioned in Subsection 2.1, depending on the problem, some reformulations and approximations are normally made to the optimal control problem formulation to address the required objectives. Here, instead of seeking the optimal control policy (i.e., $\mathbf{u}^o$), the goal is to find an optimal flight plan F^o, i.e., $(R^o, \overline{\mathrm{FL}}^o, \overline{\mathrm{M}}^o, C^o, D^o, d_D^o)$ (see Subsection 2.1.1) that minimizes the objective function given in Eq. (13) and satisfies the aircraft dynamical model (given in Eq. (6)), path and boundary constraints. Such a selection of decision space allows us to directly account for the operational restrictions, such as determining lateral routes that follow the airspace structure.

2.4.1 Ensemble trajectory integration

To determine the performance of a flight plan and evaluate the cost function Eq. (13), the corresponding trajectories of the aircraft are to be calculated using the aircraft dynamical model (provided in Subsection 2.1.1). As mentioned in Subsection 2.2, aircraft trajectories are affected by uncertainty in meteorological variables, including temperature and wind. Assuming a unique lateral path (constant course) to be tracked in practice with low-level controllers in real-time, the uncertainty in the wind (both magnitude and direction) will affect ground speed and, consequently, the time aircraft flies the route (see Fig. 6). In addition, uncertainty in temperature affects fuel consumption because the propulsive and aerodynamic performance of the aircraft and also airspeed have a dependency on temperature (Gonzalez Arribas et al., 2020). From Eq. (14), one can conclude that the uncertainty in flight time and flight mass can also affect the climate impacts (see also Fig. 5). In addition to the uncertainty in meteorological variables which is characterized using ensemble weather forecasts, uncertainty associated with initial flight conditions is taken into account within trajectory optimization problem. In this study, the initial flight time and initial mass of the aircraft are modeled as Gaussian variables, i.e., $t_0 \sim N(\bar{t}_0, \sigma_{t_0})$ and $m_0 \sim N(\bar{m}_0, \sigma_{m_0})$.

To efficiently reflect the effects of wind uncertainty in flight performance variables, instead of time, the distance flown along the route (s) is considered as the independent variable using $(\mathrm{d}t)(\mathrm{d}s)^{-1} = v_{gs}^{-1}$. This is beneficial since the uniqueness of time for all possible realizations of wind means that the position of the aircraft is fixed with respect to time. In this case, the effects of uncertainty cannot be considered efficiently because the range of feasible solutions is limited. The selection of distance flown as the independent variable allows for reflecting wind uncertainty in flight time.

According to the defined objective function (Eq. (13)), the flight performance variables required to evaluate Eq. (13) are flight time, final mass and the climate impact. By using $\mathrm{TI}(\cdot)$ to denote the integration of the aircraft dynamical model for a given flight plan, weather data, and initial flight conditions, we receive the expected final mass, the expected final time, and

https://doi.org/10.5194/egusphere-2022-1010
Preprint. Discussion started: 15 November 2022

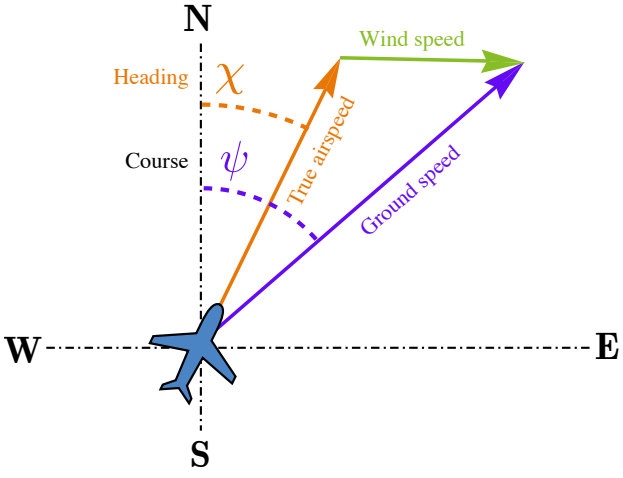

Figure 6. Relationship between wind, course, heading, airspeed, and ground speed.

the expected ATR required to evaluate the performance of aircraft trajectory (i.e., calculate the objective function given in Eq. (13)) as follows:

$$\Big[\mathbb{E}\{\mathrm{FT}\},\, \mathbb{E}\{\mathrm{FB}\},\, \mathbb{E}\{\mathrm{ATR}\}\Big] = \mathbb{E}\Big\{\mathrm{TI}(F, W, t_0, m_0)\Big\}. \tag{15}$$

In the formulated robust optimization problem, the uncertain variables are considered as continuous random variables with known probability distribution functions. As the weather variables for an ensemble weather forecast are directly represented in a discrete fashion, we assume a discrete probability distribution for the uncertainty. Considering N_{EPS} probable realizations of uncertainty (i.e., $\{\zeta_j\}_1^{N_{\mathrm{EPS}}}$), weather variables take discrete values as $\{W^1, W^2 \cdots, W^{N_{\mathrm{EPS}}}\}$, where

$$W^j := \Big[\mathrm{T}^j \quad w_x^j \quad w_y^j \quad \Phi^j \quad \mathrm{r}_{\mathrm{hum}}^j \quad \mathrm{q}^j \quad \mathrm{PV}^j \quad \mathrm{OLR}^j\Big] \tag{16}$$

is a set of meteorological variables required for climate optimal trajectory planning and $W^j(\cdot) := W(\cdot, \zeta_j)$. Generally, different members of the ensemble weather forecasts are considered equally probable. This implies that a specific forecasted weather pattern that has a higher probability will be represented by a larger number of ensemble members. Probabilistic metrics such as ensemble mean and ensemble spread use equal weights to calculate average values. In this study, we use equal weights for each probable realization of weather variables, i.e., with a probability of $\mathbf{P}(W = W^j) = N_{\mathrm{EPS}}^{-1}$. Thus, using an unweighted average between all ensemble members, Eq. (15) can be written as:

$$\Big[\mathbb{E}\{\mathrm{FT}\},\, \mathbb{E}\{\mathrm{FB}\},\, \mathbb{E}\{\mathrm{ATR}\}\Big] \approx \frac{1}{N_{\mathrm{EPS}}} \sum_{j=1}^{N_{\mathrm{EPS}}} \mathrm{TI}(F, W^j, t_0^j, m_0^j) \tag{17}$$

https://doi.org/10.5194/egusphere-2022-1010
Preprint. Discussion started: 15 November 2022

where $t_0^j, m_0^j \sim t_0, m_0$ are sampled independently, W^j is j-th member of the ensemble weather forecast, and the expected ATR is calculated as

$$\mathbb{E}\{\text{ATR}\} \approx \frac{1}{N_{\text{EPS}}} \sum_{j=1}^{N_{\text{EPS}}} \text{ATR}^j; \qquad \text{ATR}^j = \sum_{i=1}^{5} \text{ATR}_i^j$$

for $i \in \{\text{CH}_4, \text{Cont.}, \text{O}_3, \text{H}_2\text{O}, \text{CO}_2\}$. For instance, ATR^j for ozone and contrails can be calculated as

$$\text{ATR}_{\text{O}_3}^j = 10^{-3} \int_{t_0^j}^{t_f^j} \text{aCCF}_{\text{O}_3}^j\left(\mathbf{x}^j(t^j), t^j\right) \times \overbrace{FF\left(\mathbf{x}^j(t^j, t^j), \mathbf{u}^j(t^j)\right) \times \text{EI}_{\text{NO}_\text{x}}^j\left(\mathbf{x}^j(t^j), \mathbf{u}^j(t^j, t^j)\right)}^{\dot{m}_{nox}^j(t^j)} \text{d}t^j$$

$$\text{ATR}_{\text{Cont.}}^j = 10^{-3} \int_{t_0^j}^{t_f^j} \text{aCCF}_{\text{Cont.}}^j\left(\mathbf{x}^j(t^j), t^j\right) v_{gs}^j(t^j) \text{d}t^j = 10^{-3} \int_0^{s_f} \text{aCCF}_{\text{Cont.}}^j\left(\mathbf{x}^j(t^j(s)), t^j(s)\right) \text{d}s \tag{18}$$

where $\mathbf{x}^j(t^j)$ and $\mathbf{u}^j(t^j)$ are the state and control variables of the aircraft considering j-th realization of weather variables and j-th sampled initial conditions, $\text{d}s = v_{gs}^j \cdot \text{d}t^j$, and

$$\begin{aligned}
\text{aCCF}_{\text{O}_3}^j(\mathbf{x}^j(t^j), t^j) &:= \text{aCCF}_{O_3}\left(\text{T}^j\left(\mathbf{x}^j(t^j), t^j\right), \Phi^j\left(\mathbf{x}^j(t^j), t^j\right)\right) \\
\text{aCCF}_{\text{Cont.}}^j(\mathbf{x}^j(t^j), t^j) &:= \text{aCCF}_{\text{Cont.}}\left(\text{T}^j\left(\mathbf{x}^j(t^j), t^j\right), \text{OLR}^j\left(\mathbf{x}^j(t^j), t^j\right), \text{r}_{\text{hum}}^j\left(\mathbf{x}^j(t^j), t^j\right)\right)
\end{aligned} \tag{19}$$

where the weather variables such as T^j, Φ^j are j-th members of the ensemble weather forecast. The actual NO_x emission index, i.e. $\text{EI}_{\text{NO}_\text{x}}^j\left(\mathbf{x}^j(t^j), \mathbf{u}^j(t^j)\right)$ is calculated using BFFM2. As can be seen in Eq. (18), the climate impact due to the NO_x emission depends on the amount of NO_x emitted in NO_x-sensitive regions, while for contrails, it depends on the distance flown in persistent contrail formation areas.

Heun's method is adopted for integrating the aircraft dynamical model along discretized segments of the route through each phase, i.e., climb, descent, and cruise (Gonzalez Arribas et al., 2020). Since the calculations are similar for different members, parallelization would be beneficial in reducing computational time. Here, CUDA (Guide, 2013; Klöckner et al., 2012), a tool for general-purpose computing on the graphics processing unit, is employed to ~~parallel~~ the computations.

2.4.2 Performance evaluation of a flight plan

The expected values obtained from Eq. (17) are for a specific flight plan. By these settings, for this flight plan, the cost function given in Eq. (13) can be evaluated with the following equation

$$J(F) = \psi_{\text{CST}}\left[\psi_t \cdot \mathbb{E}\{\text{FT}\} + \psi_m \cdot \mathbb{E}\{\text{FB}\}\right] + \psi_{\text{CLM}} \cdot \mathbb{E}\{\text{ATR}\}. \tag{20}$$

Figure 7 shows how the expected performance is calculated and evaluated for a given flight plan and an ensemble weather forecast. The objective is to find a flight plan that minimizes Eq. (20). Since the flight plan includes both discrete and continuous decision variables, the optimizer should be capable of solving the optimization within the hybrid decision spaces. A classical

https://doi.org/10.5194/egusphere-2022-1010
Preprint. Discussion started: 15 November 2022

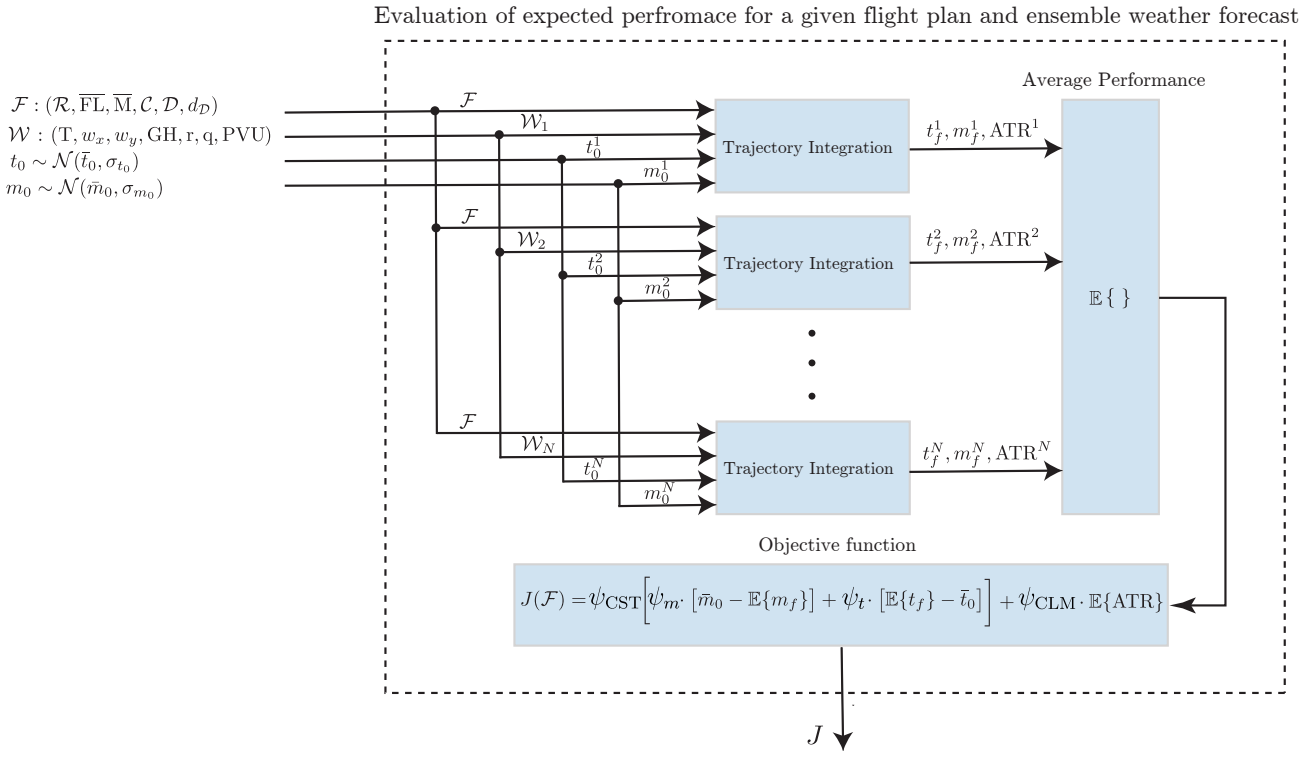

Figure 7. Calculation and evaluation of the expected performance for a given flight plan and an ensemble weather forecast.

approach to solving such optimization problems is mixed-integer nonlinear programming, which is mathematically complex and computationally intensive.

2.4.3 Probabilistic flight plan generation

To solve the optimization with hybrid decision variables in an efficient manner, instead of directly searching for the optimal flight plan, the optimization is conducted in the space of probability distributions defined over flight plans. In other words, instead of directly minimizing $\min_F J(F)$, the minimization of the following equivalent problem is considered

$$\min_{p(F)} \mathbb{E}_{p(F)}[J(F)] \tag{21}$$

which provides the same optimal solution, i.e., if F^* is the optimal solution to the original problem, $\mathbf{P}(F = F^*) = 1$ provides the same results. The optimization is carried out in the space of probability distributions to move to continuous search space. In addition, it can facilitate searching by parameterizing the distribution p with a parameter vector $\theta \in \mathbb{R}^{\Theta}$, approximating Eq. (21) as

$$\min_{\theta} \mathbb{E}_{p(F;\theta)}[J(F)] \tag{22}$$

https://doi.org/10.5194/egusphere-2022-1010
Preprint. Discussion started: 15 November 2022

which generally is not identical to Eq. (21), as it relies on whether the parameterization is able to capture a distribution where $\mathbf{P}(F = F^*) = 1$. Thus, the parameterization of the distribution p using the vector θ plays an important role in approximating the original problem. In Gonzalez Arribas et al. (2020), the Probabilistic-execution Flight Plan (PF) is introduced to parameterize the distribution over the space of possible flight plans. In this approach, the parameter vector θ is defined as follows:

$$\theta = \begin{bmatrix} \Upsilon^T & \hat{\mathrm{M}}^T & \hat{\mathrm{FL}}^T & \hat{C}^T & \hat{D}^T & d_D^T \end{bmatrix}^T \in \mathbb{R}^{\Theta} \tag{23}$$

where $\Upsilon \in \mathbb{R}^{n_{sp}}$ is a vector assigning probability to select each airway, and $\hat{\mathrm{M}}$, $\hat{\mathrm{FL}}$, $\hat{C}$, $\hat{D}$, and d_D are the parameterized Mach schedule, flight level, climb profile, descent profile and distance-to-go, respectively. For a parameter vector θ of a PF, flight plans can be randomly generated. For instance, let us explain how the lateral path is sampled from a given vector of parameters Υ. First, assume that all waypoints of the graph are processed and limited to two outgoing airways. This can be done by considering virtual edges of zero length for those waypoints with more than two outgoing airways. The vector composed by a set of junctions is defined as $\bar{V} = \{v_k\}_{k=1}^{n_{sp}} \in \mathbb{R}^{n_{sp}}$. At k-th junction waypoint, the selection of airway is done through a random process: for k-th entry of a given vector Υ (i.e., v_k), and k-th entry of a vector containing uniform random variables $\xi_k (\in \Xi \sim U(0,1))$, the airway is selected as:

$$\text{selected airway at } k\text{-th junction waypoint} = \begin{cases} \text{airway 1} & \mathrm{S}(v_k) \leq \xi_k \\ \text{airway 2} & \mathrm{S}(v_k) > \xi_k \end{cases}$$

where $\mathrm{S}(\cdot)$ is a sigmoid function: $\mathrm{S}(x) = 0.5[1 + x(\sqrt{1+x^2})^{-1}]$. Therefore, for a given vector of parameters Υ and a given vector of random variables, a lateral path (restricted to the structure of airspace) can be sampled. The approach to sampling a complete flight plan from $p(F;\theta)$, such as sampling Mach schedule and flight level, is presented in Gonzalez Arribas et al. (2020) (see Algorithm 1). It is worth mentioning that the operational aspects and feasibility of the aircraft trajectory are considered within the generation of flight plans. For instance, continuous Mach adjustment is avoided, and flight level changes' frequency is limited.

2.4.4 Optimization: augmented random search

In the probabilistic-execution flight plan approach, to sample the flight plan from a given θ, vectors containing random variables are required. Thus, the PF associated with θ is stochastic. To evaluate $\mathbb{E}_\theta[J(F)] := \mathbb{E}_{p(F;\theta)}[J(F)]$ for a given θ, sampling of multiple flight plans is required. By generating N_{FP} sets of random variables, N_{FP} flight plans (i.e., F_j for $j = 1, \cdots, N_{\mathrm{FP}}$) can be sampled independently for a given θ. To benefit from the provided N_{EPS} probable realizations of meteorological variables, and N_{EPS} samples of exogenous sources of uncertainty (i.e., initial flight time and initial flight mass), we sample N_{EPS} (i.e., $N_{\mathrm{FP}} = N_{\mathrm{EPS}}$) potential flight plans for a given θ. In other words, each sampled flight plan is evaluated with one realization of meteorological conditions. In this respect, one can rewrite Eqs. (17,20) as:

$$\left[\widehat{\mathrm{FT}},\ \widehat{\mathrm{FB}},\ \widehat{\mathrm{ATR}}\right] = \frac{1}{N_{\mathrm{EPS}}} \sum_j \mathrm{TI}(F_j, W^j, t_0^j, m_0^j)$$

https://doi.org/10.5194/egusphere-2022-1010
Preprint. Discussion started: 15 November 2022

$$\mathbb{E}_\theta[J(F)] \approx \hat{J} := \psi_{\text{CST}}\left[\psi_t \cdot \widehat{\text{FT}} + \psi_m \cdot \widehat{\text{FB}}\right] + \psi_{\text{CLM}} \cdot \widehat{\text{ATR}}. \tag{24}$$

The flight planning problem can now be expressed as the following stochastic optimization problem:

$$\min_\theta \mathbb{E}[\hat{J}] \tag{25}$$

where the objective is to find the optimal value of θ (which parametrizes the probability distribution $p(F;\theta)$) such that a population of randomly sampled flight plans minimizes the expected cost Eq. (25). Sampling N_{EPS} flight plans and using them in a pair-wise manner with ensemble members for trajectory integration to evaluate Eq. (24) is computationally more efficient than sampling a different number of flight plans ($N_{\text{FP}} \neq N_{\text{EPS}}$) and then evaluating each sampled flight plan with all the ensemble members. This is because, in this case, we only integrate the aircraft trajectory N_{EPS} times instead of performing $N_{\text{FP}} \times N_{\text{EPS}}$ trajectory integrations. In spite of reducing the number of computations, it provides similar results. This is due to the fact that, despite sampling multiple flight plans for the evaluation of the objective function Eq. (24) for a given θ, as the process goes by, all flight plans converge to a unique flight plan. For instance, let us consider the process of sampling the lateral path presented in Subsection 2.4.3. The choice of each airway relies on two parameters: υ and ξ. For the first iterations of the optimization algorithm, all outgoing airways from waypoints are almost equally probable. However, with more iterations, the decision variable θ is improved, leading to increasing or decreasing the parameter υ. This parameter converges to a large positive or negative value for the last iterations. For instance, in the case of large υ, $\lim_{\upsilon\to\infty} \text{S}(\upsilon_k) = 1$, implying $\text{S}(\upsilon_k) \geq \xi_k$ for all the sampled flight plans. Thus, in the end, for the optimal value of θ obtained from optimization, we receive a unique flight plan. In this case, for the similar flight plans that are sampled for the last iterations, the expected flight performance variables obtained (from Eq. (24)) using $N_{\text{FP}} \times N_{\text{EPS}}$ and N_{EPS} times trajectory integration will be almost the same.

In this work, the V1 version of the Augmented Random Search (ARS) algorithm adopted from (Mania et al., 2018; Gonzalez Arribas et al., 2020) is employed. This is a gradient-like algorithm in which, it starts from an initial point θ_0, then generates n random search directions $\omega \in \mathbb{R}^\Theta$. In the next step, it evaluates $\hat{J}^+ := \hat{J}(\theta + \mathbf{S}\omega)$ and $\hat{J}^- := \hat{J}(\theta - \mathbf{S}\omega)$, where $\mathbf{S} \in \mathbb{R}^{\Theta\times\Theta}$ is a diagonal matrix, adjusting the relative variations that are allowed between decision variables. Then, the decision variables θ are improved along all search directions proportional to $\hat{J}^+ - \hat{J}^-$. The algorithms, details on the optimization approach, and also parallelization on GPUs are provided in (Gonzalez Arribas et al., 2020).

3 Results

The effectiveness of the proposed optimization algorithm to plan robust climate optimal aircraft trajectories with respect to uncertain meteorological conditions is analyzed for a flight from Frankfurt to Kyiv on two different days and departure times:

- **Scenario 1**: 13$^{\text{th}}$ of June 2018, 0000UTC, a scenario in which aircraft flies through areas favorable for the formation of persistent contrails.
- **Scenario 2**: 10$^{\text{th}}$ of December 2018, 1200UTC, a scenario with no formation of persistent contrails.

https://doi.org/10.5194/egusphere-2022-1010
Preprint. Discussion started: 15 November 2022

Table 2. The data obtained from the ICAO databank to calculate the actual emission index of Airbus model A320-214, with the engine CFM56-5B4/P.

Parameter	Value	Unit	Description
FF_{ref}	1.132, 0.935, 0.312, 0.104	[kg/s]	Reference fuel flow at take-off, climb out, approach, and idle conditions, respectively.
$\mathrm{EI}_{\mathrm{NO_x},ref}$	28, 23.2, 10, 4.3	[g/kg]	Reference $\mathrm{NO_x}$ emission index at take-off, climb out, approach, and idle conditions, respectively.
r	1.010, 1.013, 1.02, 1.1	-	Boeing adjustment factor for take-off, climb out, approach, and idle conditions, respectively (DuBois and Paynter, 2006).

The dominant climate impact of contrails is the main reason for selecting these two scenarios, providing better insight into the mitigation potentials.

For the route graph, the full airspace graph of the considered days is filtered and processed to include all paths from the end of the standard instrument departures of the origin airport to the beginning of the standard instrument arrivals of the destination airport with the maximum length of 104% of the shortest path length. The considered aircraft is an Airbus, model A320-214, with the engine CFM56-5B4/P. Table 2 provides the required parameters to calculate the $\mathrm{NO_x}$ emission index of the considered aircraft using BFFM2. The initial flight time and initial mass are modeled as Gaussian variables: $t_0 \sim N(0000\ \mathrm{UTC}, 10)$[s] for Scenario 1, $t_0 \sim N(1200\ \mathrm{UTC}, 10)$[s] for Scenario 2, and $m_0 \sim N(61600, 10)$[kg]. As for meteorological input data, due to ease of availability, the ERA5 Reanalysis data products containing ten ensemble members are adopted for this study. It is worth mentioning that forecast data with more ensemble members can be employed similarly.

The weighting parameters of the objective function given in Eq. (7) are selected as: $\psi_{\mathrm{CST}} = \alpha$ [-] and $\psi_{\mathrm{CLM}} = (1-\alpha)\mathrm{K}$ [USD/K], where K is a scaling (or conversion) factor determined as

$$\mathrm{K} = \frac{\mathrm{SOC_{climate}} - \mathrm{SOC_{cost}}}{\mathrm{ATR_{cost}} - \mathrm{ATR_{climate}}} \tag{26}$$

where for instance, $\mathrm{SOC_{climate}}$ is the SOC calculated when the optimization objective is only the climate impact or $\mathrm{ATR_{cost}}$ is the ATR when the objective is only SOC. $\alpha \in [0,1]$ is a weighting parameter that penalizes cost versus climate impact in which $\alpha = 0$ is the pure cost optimal and $\alpha = 1$ is the pure climate optimal routing strategies. In the simulations, we consider five different values for α in order to explore the trade-off between operating cost and climate impact represented by SOC and ATR, respectively.

3.1 Scenario 1: formation of persistent contrails

We consider a scenario in which the aircraft flies through warming contrails for the cost optimal routing option. Before presenting the results, the performance of the proposed optimizer in terms of convergence and computational time is analyzed. Since the optimization approach is stochastic, different results may be obtained with different executions. To explore the sensitivity

https://doi.org/10.5194/egusphere-2022-1010
Preprint. Discussion started: 15 November 2022

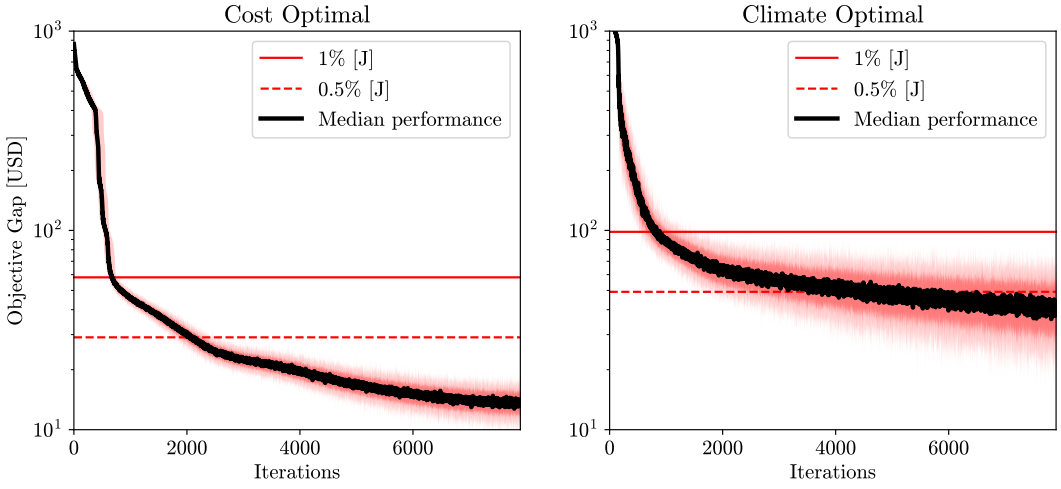

Figure 8. Sensitivity of the convergence performance of the optimization algorithm to 50 different executions for the cost and climate optimal routing options ($\alpha = 1$ and $\alpha = 0$, respectively)(1 iteration $\approx$ 4 ms). The objective gap is calculated considering the deviations from the best performance obtained among 50 runs (i.e., the minimum value of J) as the reference, i.e., at each iteration, the value of the objective function (used for trajectory optimization Eq. (24)) is compared with the minimum value obtained from other executions. The mean value is highlighted in a solid black line, and 0, 10, 90, and 100 percentiles are represented with different color bands.

of the optimization method, 50 different runs are performed with similar settings for pure cost (i.e., $\alpha = 1.0$) and pure climate optimal (i.e., $\alpha = 0.0$) routing options. Then, the objective gap is calculated considering the best performance obtained from different solutions (i.e., the minimum value of J) as the reference. The convergence performances with averaged values as solid lines and 0, 10, 90, and 100 percentiles are depicted in Fig. 8. For both cases, with around 700 iterations ($\approx 2.8s$) for the cost optimal trajectory and 900 iterations ($\approx 3.6s$) for the climate optimal one, the estimated objective gaps quickly reduce up to 1% of the values of the objective functions J. As the climate optimal routing option is associated with the inclusion of aCCFs calculated from meteorological variables, the optimization is much more complex, which can be validated in Fig. 8. With around 4000 iterations ($16s$), the objective gap is reduced up to 0.5% of J. Consequently, with a maximum of 4000 iterations, near-optimal performance can be obtained with +0.5% maximum deviation around the best-obtained value (i.e., the most optimal case).

Now, we proceed to present the obtained results. The aircraft profiles and climate responses for different routing options are given in Fig. 9. The SOC depends on the flight time and fuel consumption. Therefore, the aircraft for routing strategies with higher values of α, such as $\alpha = 1.0, 0.8$, tends to fly at higher altitudes within the vertical constraints because flying at higher altitudes is beneficial to reducing fuel consumption, which contributes a large part of the total operating cost (see Fig. 9a). By analyzing the lateral paths depicted in Fig. 10 with the direction and speed of wind at different flight levels, one can see that aircraft deviates from the shortest path to benefit from stronger tailwinds. For trajectories with lower climate impacts, as can be seen in Fig. 9a, the aircraft flies at relatively lower altitudes compared to the cost optimal routing option mainly to

https://doi.org/10.5194/egusphere-2022-1010
Preprint. Discussion started: 15 November 2022

avoid the formation of persistent contrails (due to warming impacts during nighttime). The climate optimal routing options reduce the warming effect of contrails. Although the warming climate effects of NO_x emission and water vapor increase with climate optimal trajectories, the net climate impact decreases. This is because the climate impact of contrails outweighs the impact associated with other species (as discussed in Subsection 2.1.2). The contribution of each species to total climate impact, variability of the obtained climate impacts and SOC with ranges of uncertainty for different α's, and Pareto-frontiers are provided in Fig. 11. For a specific case ($\alpha = 0.2$), by accepting an increase of 4% in cost, there is a potential to mitigate the climate impact by 55% considering median performance. In Subsection 2.2, it was shown that the variability of relative humidity among ensemble members is high, leading to high uncertainty in the aCCF of contrails. As expected, the obtained climate impact of contrails is highly uncertain when the aircraft flies through areas sensitive to form persistent contrails. In contrast, as the aircraft tends to avoid PCFA, the ranges of uncertainty reduce, in which, for the complete avoidance that is achieved with $\alpha = 0.2$, the climate impact is almost deterministic. In addition, SOC requires flight time and fuel consumption to represent operating cost in USD, and as it is affected by relatively less uncertain meteorological variables (i.e., wind and temperature compared to relative humidity for the considered case study as analyzed in Subsection 2.2), the uncertainty in its value is small.

https://doi.org/10.5194/egusphere-2022-1010
Preprint. Discussion started: 15 November 2022

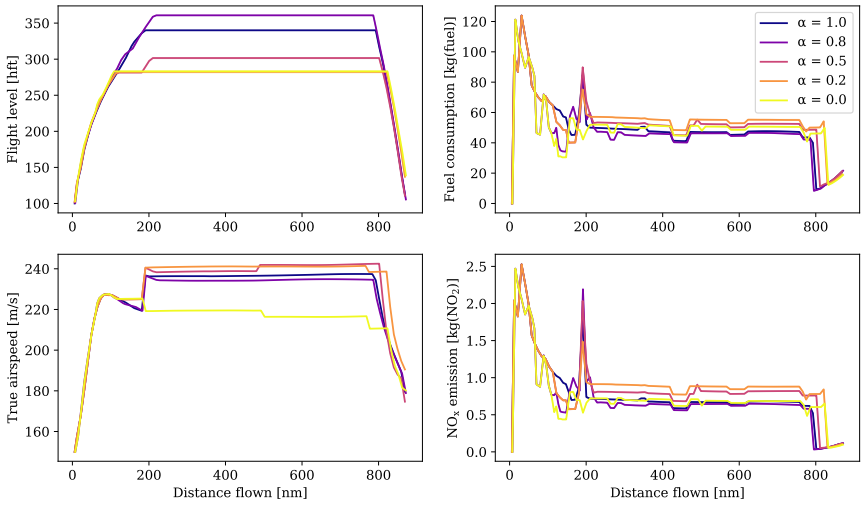

(a) Flight level, fuel consumption, true airspeed, and NO_x emission.

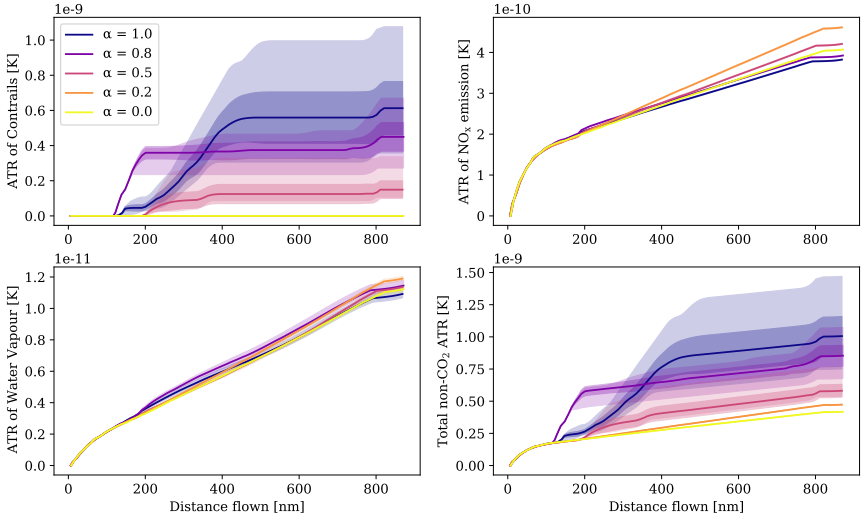

(b) ATR of persistent contrails, ATR of NO_x emission, ATR of water vapor emission, and net ATR of non-CO_2 emissions (accumulated values along the route).

Figure 9. Results of Scenario 1 (13th of June 2018, 0000UTC) for different routing options (i.e., α's). The shaded regions show the ranges of uncertainty associated with uncertain meteorological conditions (outer lighter areas show the minimum and maximum values while the inner darker ones represent 95% confidence interval).

By analyzing the contribution of each species to the net ATR for different α's, one can conclude that the mitigation potential is achieved mainly by avoiding contrails-sensitive areas, which result in slight increases in the climate of NO_x emission (see Fig. 11a). However, when the formation of persistent contrails is completely avoided (i.e., with $\alpha = 0.2$), the optimizer tends to reduce NO_x emission mainly by reducing speed to reduce the fuel flow required to calculate NO_x emission index and also

https://doi.org/10.5194/egusphere-2022-1010
Preprint. Discussion started: 15 November 2022

total NO_x emission (i.e., NO_x emission = NO_x emission index * fuel consumption). Reducing NO_x emission by flying at lower speeds is achieved at the expense of a considerable increase in flight time and, consequently, SOC. As can be concluded from Pareto frontiers, such a reduction in climate impact for this scenario is not cheap as only 5% more reduction in climate impact is obtained with almost 4% more increase in SOC (α = 0.0). As the aCCF of contrails is only evaluated in areas favorable for the formation of persistent contrails, typically determined using inequality constraints, it has sharp spatial behaviors (i.e., PCFA (latitude, longitude, altitude, time) $\in$ { 0, 1 }). In addition, contrails have dominant climate effects. Therefore, the optimizer's first choice is to avoid forming persistent contrails, which may be achieved more efficiently than reducing the impacts of other species with relatively lower climate impacts and smooth spatial behaviors. This can be validated in Fig. 11a as the lowest priority is given to reducing the climate impact associated with NO_x emission (for $\alpha = 0$).

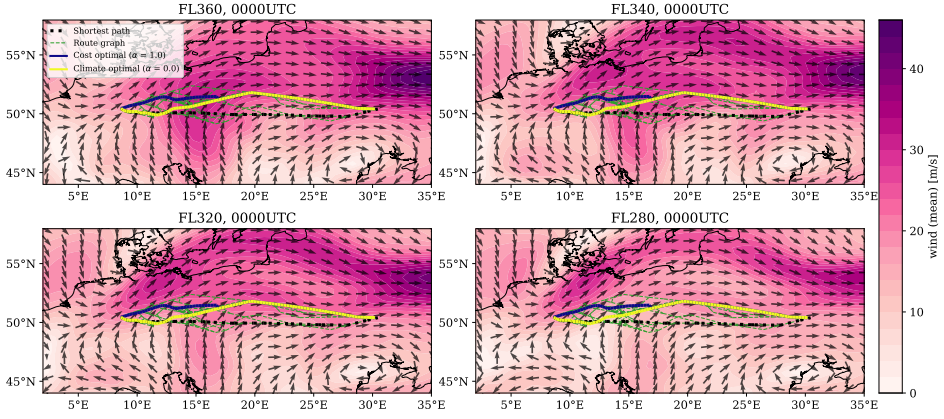

(a)

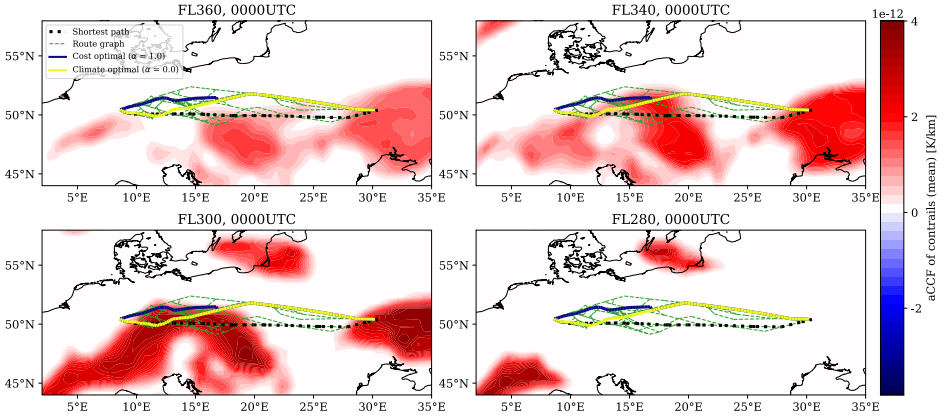

(b)

Figure 10. Lateral paths for Scenario 1 (13th of June 2018, 0000UTC) depicted with (a) wind and (b) aCCF of contrails as colormaps.

https://doi.org/10.5194/egusphere-2022-1010
Preprint. Discussion started: 15 November 2022

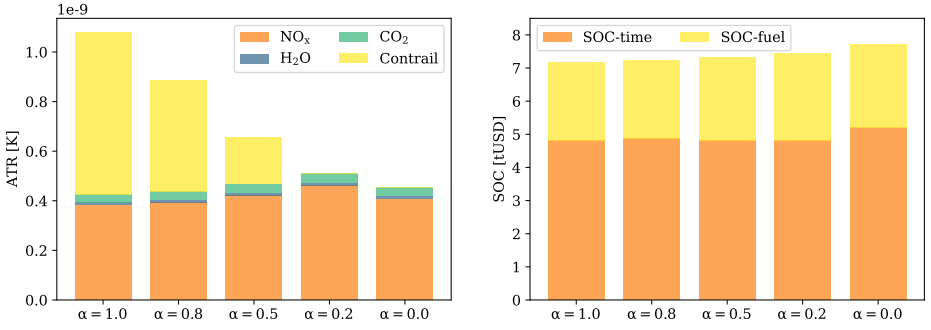

(a) Contribution of each species to the net ATR, and costs of flight time and fuel consumption to the net SOC (mean values).

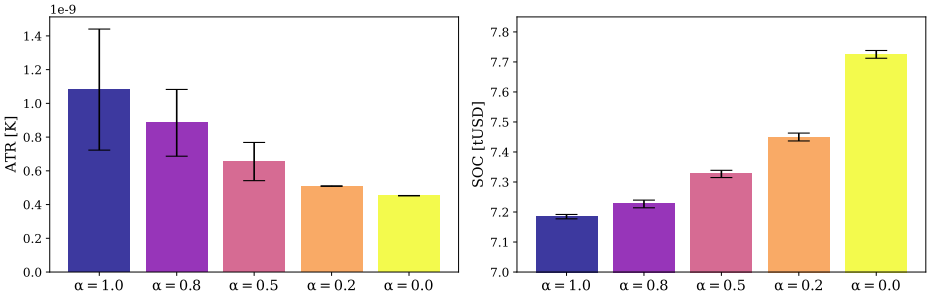

(b) ATR and SOC with ranges of uncertainty (min-max) for different routing options.

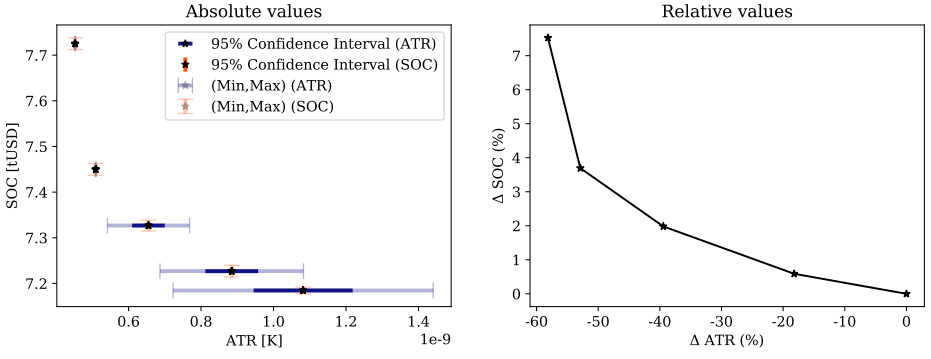

(c) Pareto-frontiers considering absolute and relative values.

Figure 11. Overall performance of the optimized trajectories in terms of ATR and SOC for Scenario 1 (13th of June 2018, 0000UTC).

3.2 Scenario 2: no formation of persistent contrails

In the next scenario, we analyze the mitigation potential when no persistent contrails are formed with the cost optimal routing option.

https://doi.org/10.5194/egusphere-2022-1010
Preprint. Discussion started: 15 November 2022

For this case, aircraft profiles and climate responses are depicted in Figs. 12a, 12b, respectively. As can be seen in Fig. 12a, the optimizer chooses to fly at lower altitudes for routing strategies with higher penalization on climate impact. As no persistent contrails are formed (see Fig. 13a), we depict the lateral paths with the merged aCCFs (calculated using the mean values of the obtained NO_x emission index) as the colormap at different flight levels in Fig. 13b. As can be seen, flying at lower altitudes is more beneficial in reducing the climate impact of other species (mainly NO_x). In addition to lowering cruise altitude, the aircraft flies at lower speeds to reduce the fuel flow and, consequently, fuel consumption, NO_x emission index, and NO_x emission. The variability of climate impact and SOC for different α's and Pareto frontiers are given in Fig. 14. By reducing α, the climate impact decreases at the cost of an increase in SOC. For instance, for $\alpha = 0.2$, by accepting a 0.8% increase in cost, a 15% reduction in ATR can be achieved. As in the previous case, the relative increase in SOC is considerable for $\alpha = 0$ since the aircraft tends to fly at a relatively lower speed for more reduction in climate impact.

In conclusion, climate impact reduction is achieved at the expense of a higher cost increase than in the previous scenario. Moreover, since no contrails are formed, the uncertainty in climate impact is almost neglectable.

https://doi.org/10.5194/egusphere-2022-1010
Preprint. Discussion started: 15 November 2022

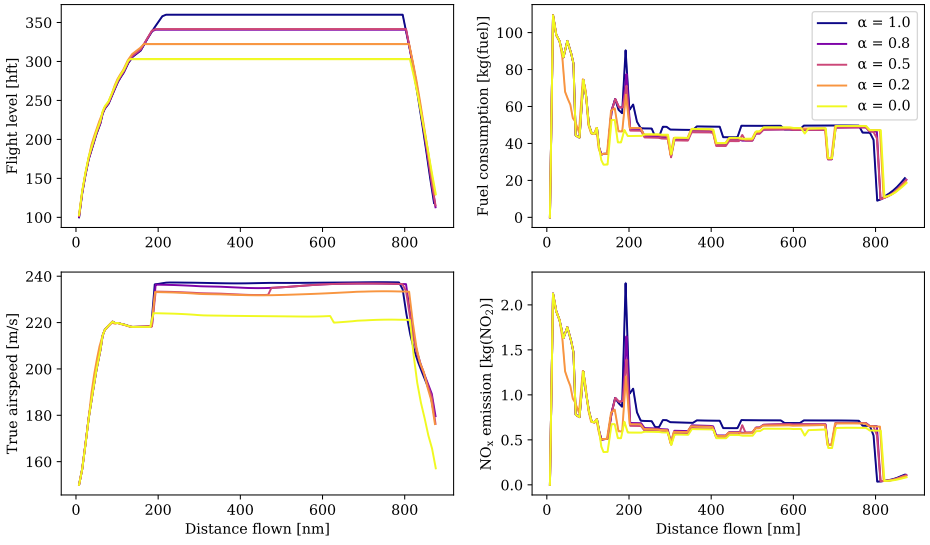

(a) Flight level, fuel consumption, true airspeed, and NO_x emission.

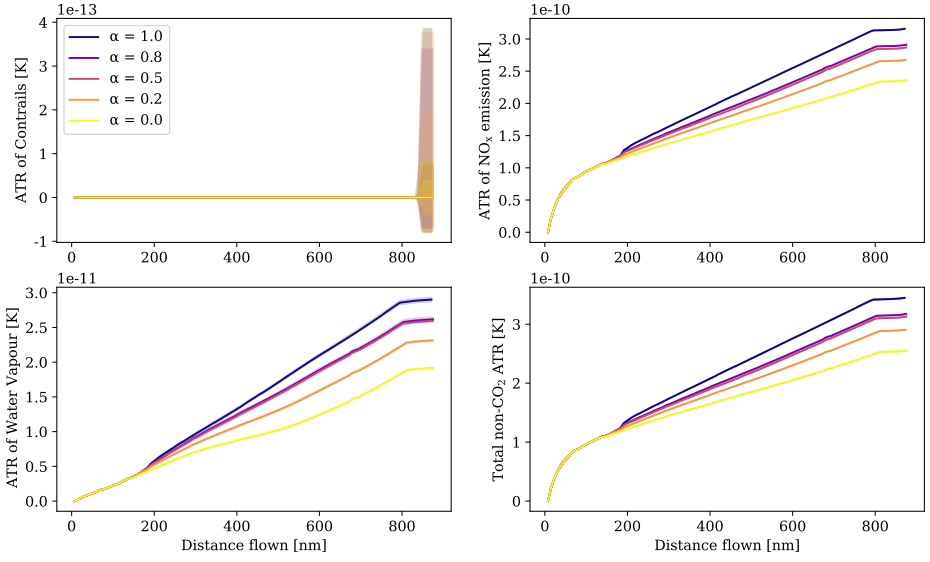

(b) ATR of persistent contrails, ATR of NO_x emission, ATR of water vapor emission, and net ATR of non-CO_2 emissions (accumulated values along the route).

Figure 12. Results of Scenario 2 (10^{th} of December 2018, 1200UTC) for different routing options (i.e., α's). The shaded regions show the ranges of uncertainty associated with uncertain meteorological conditions (outer lighter areas show the minimum and maximum values while the inner darker ones represent 95% confidence interval).

https://doi.org/10.5194/egusphere-2022-1010
Preprint. Discussion started: 15 November 2022

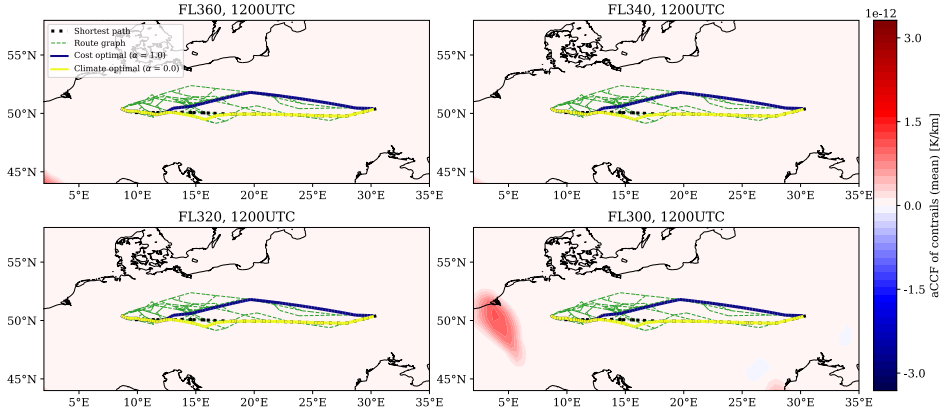

(a)

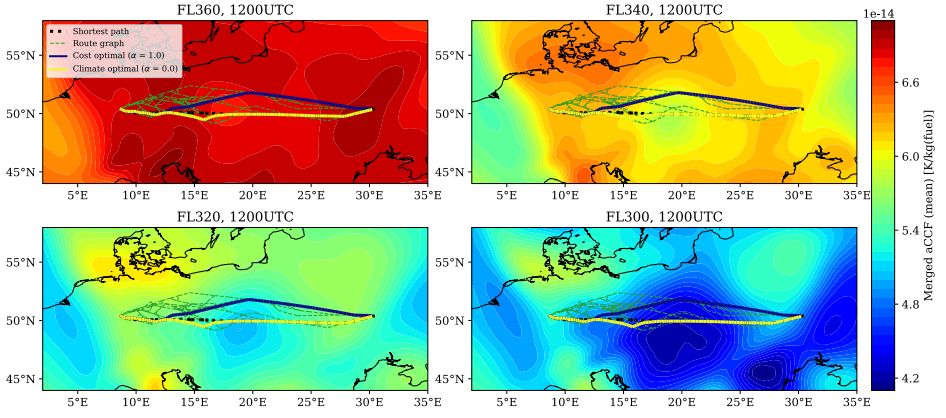

(b)

Figure 13. Lateral paths with (a) aCCF of contrails and (b) merged aCCFs as colormaps at different flight levels for Scenario 2 (10^{th} of December 2018, 1200UTC).

https://doi.org/10.5194/egusphere-2022-1010
Preprint. Discussion started: 15 November 2022

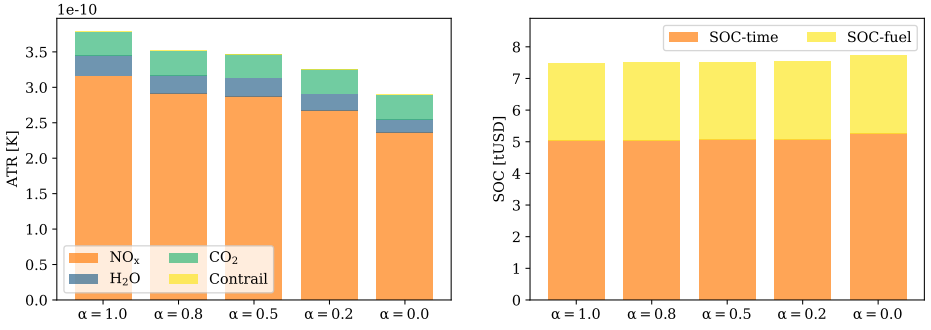

(a) Contribution of each species to the net ATR, and costs of flight time and fuel consumption to the net SOC (mean values).

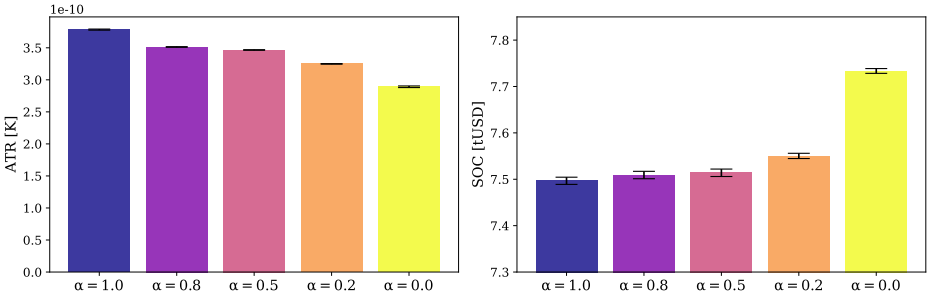

(b) ATR and SOC with ranges of uncertainty (min-max) for different routing options.

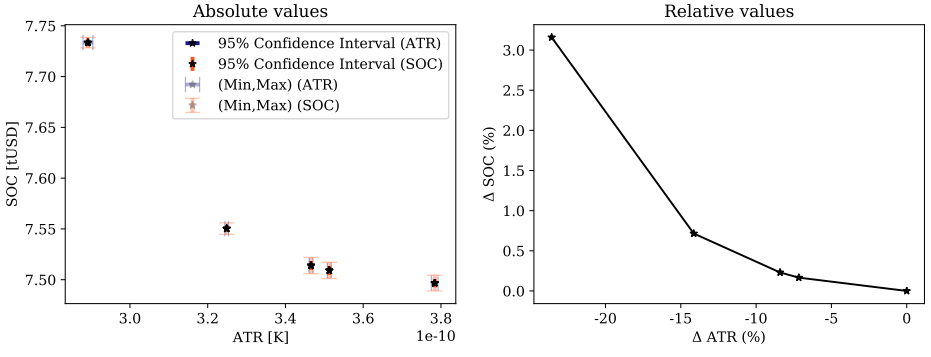

(c) Pareto-frontiers considering absolute and relative values.

Figure 14. Overall performance of the optimized trajectories in terms of ATR and SOC for Scenario 2 (10^{th} of December 2018, 1200UTC).

4 Discussion

This paper presented a methodology to plan robust climate optimal aircraft trajectory under uncertain meteorological conditions. Discussion on the obtained results and some general remarks are presented in the following.

https://doi.org/10.5194/egusphere-2022-1010
Preprint. Discussion started: 15 November 2022

The obtained mitigation potentials for the considered scenarios were different due to the variability of meteorological conditions. In both cases, the climate optimal routing options could reduce the climate impacts. The cost optimal trajectories flew at higher altitudes compared to climate optimal ones, as flying at higher altitudes is beneficial to reducing fuel consumption. This is also in line with related studies in the literature (e.g., (Yamashita et al., 2020)). Due to the dominant climate impact and non-smooth spatial behavior of contrails, the mitigation potential obtained for the scenario with contrails effects (i.e., scenario 1) was higher than the scenario with no formation of persistent contrails. The non-smooth spatial behavior of contrails' climate impact is related to the conditions of PCFA. Due to the high variability among the ensemble members of relative humidity over ice needed to determine PCFA, the climate impact of contrails was highly uncertain. However, for the cases ~~with no contrails' climate effect~~, the total climate impact was almost deterministic. This is because the variability in the other weather variables was neglectable. For both scenarios, α = 0.2 seems to be a reasonable choice since the climate impacts were reduced at the expense of acceptable increases in the operating cost, and the results were almost deterministic.

In spite of considering the ensemble members in trajectory planning, a unique flight plan is determined. This reflects the operational feasibility and applicability of this method since, in the flight planning context, it is required to determine a unique lateral route in latitude and longitude that starts and ends at predefined points in space and follows the real structure of airspace as well as having a fixed altitude profile and a fixed airspeed schedule. In this case, the effects of uncertainty are reflected in the aircraft performance variables. For instance, let us consider the first scenario. For $\alpha = 1.0$, the lateral path, speed schedule, and flight level were determined in a cost optimal manner (see Figs. 9a, 10). In our approach, the optimized trajectory is assumed to be tracked as close as possible in practice with the system's low-level controllers in real-time. Aiming at optimizing a unique flight plan, the proposed method provides some ranges for the aircraft performance variables, such as fuel consumption, flight time, and climate impact, due to different probable realizations of weather conditions. For instance, the climate impact is expected to lie within the determined ranges (see Fig. 9b) if the considered ensemble members could acceptably predict future weather conditions.

In this study, we only considered the minimization of the expected performance, e.g., expected climate impact. However, the concept of robustness is mainly related to having less uncertain results (i.e., minimizing also the uncertainty range). In the case of robustness to meteorological uncertainty, we need to find a flight plan that avoids those areas of airspace with high variability among the ensemble members. For instance, in (González-Arribas et al., 2018), the dispersion on the arrival time is minimized by avoiding the regions with high variability among the ensemble members of wind (characterized by STD). In this study, we observed that the most uncertain variable is the climate impact of contrails. Since, for both scenarios, only warming contrails were formed, minimization of the expected values directly led to avoiding uncertain PCFA, and as can be seen from the results, for the climate optimized trajectories, we obtained robust solutions (almost deterministic results). However, during the daytime, different behavior is expected for the cases with the cooling contrails. This is because, to reduce the expected climate impact, aircraft will tend to fly in uncertain PCFA to benefit from cooling effects. In the next versions of ROOST, such scenarios will be taken into account, and controlling the dispersion on all flight performance variables will be addressed by including their variance in addition to the averaged values as objectives in the objective function.

https://doi.org/10.5194/egusphere-2022-1010
Preprint. Discussion started: 15 November 2022

Regarding the computational time and convergence performance, it was shown that it is scenario-dependent. For more complex problems, such as the case ~~that included~~ climate impacts quantified using aCCFs, the optimizer required more iterations to enhance the convergence compared to the cost optimal routing option. It is worth mentioning that the distance between the origin and destination, available route graphs, and also parameters within the optimization algorithm can change the convergence performance and computational time. The number of iterations is a user-defined parameter that needs to be specified based on the required performance and availability of computational resources. In the performed simulations, we considered 4000 iterations. By looking at the Pareto frontiers, it is clear that the optimizer was able to find near-optimal solutions. Thanks to the parallelization on GPUs, the computational time for achieving a near-optimal solution is promising. There exist several controlling parameters within the optimization algorithm of ROOST, including the number of search directions, the augmented random search (ARS) step size, and the Nesterov velocity factor (see (Gonzalez Arribas et al., 2020) for a description of these controlling parameters) that can affect the convergence performance. As a future work, we aim to study the effects of all these parameters and propose an optimal selection of them. Moreover, adaptive (scenario-dependent) stopping criteria will be proposed helping to optimize aircraft trajectories more efficiently in the sense of computational time.

To explore the trade-off between climate impact and the operating cost, Pareto frontiers were generated. By changing the weighting parameter α, different Pareto optimal solutions were obtained. However, with this approach, a specific value for α does not necessarily result in a similar cost increase and climate impact mitigation potential for different scenarios (e.g., for $\alpha = 0.2$, the climate impact is reduced by 55% and 15% by accepting 4% and 0.8% increase in the operating cost for scenarios 1 and 2, respectively). This approach is suitable for analyzing the mitigation potential for a single flight. However, it is not the most efficient way to study the Pareto optimal solutions of the aggregated results of a large number of flights. For such cases, having the flexibility to directly optimize flights requesting a certain range reduction in climate impact or allowing a specific range for the increased operating costs would be beneficial. In this respect, one can aggregate those climate optimal trajectories, having, for instance, a ~~+~~0.5% to ~~+~~1.0% increase in the operating cost. In future versions of ROOST, we will add this feature to the optimization tool by defining some path constraints. Such an aggregation of results is doable with α, however, one needs to generate more points in the Pareto frontier in order to classify the results based on a certain percentage increase in cost or a percentage decrease in climate impact. Scaling up this trajectory level analysis to the network scale will increase the computational time by a factor of the considered α's.

As was explored in the paper, the mitigation of climate impact within the flight planning context is achieved only by accepting some extra costs due to avoidance of highly climate-sensitive regions, which is in line with related studies in the literature (e.g., (Yamashita et al., 2020, 2021; Lührs et al., 2021; Niklaß et al., 2019)). An alternative for the compensation of such additional costs is to consider fees and taxes for the aviation-induced climate impact in order to motivate airliners to adopt climate optimal trajectories. Currently, there is no climate policy for the aviation non-CO_2 climate effects in the planned market-based instruments such as the emission trading scheme (ETS). However several studies have proposed frameworks to include costs of aviation-induced non-CO_2 climate effects into the operating cost, such as the concept of equivalent CO_2 emissions and the concept of climate-charged airspace (Niklaß et al., 2021). If taxes are applied to the non-CO_2 climate effects, climate optimal trajectories can also be economically beneficial.

https://doi.org/10.5194/egusphere-2022-1010
Preprint. Discussion started: 15 November 2022

The aCCFs used in this study represent a prototype formulation. The aCCF algorithms were developed for meteorological summer and winter conditions with a focus on the North Atlantic flight corridor. Thus, the usage of the aCCFs for different seasons and regions needs special caution. However, further development of the aCCFs and an expansion of their geographic scope and seasonal representation is ongoing research.

5 Conclusions

This paper addressed the problem of determining robust climate optimal aircraft trajectory within the structured airspace under uncertain meteorological conditions. The climate-sensitive regions were identified using the prototype algorithmic climate change functions version 1.1. The ensemble prediction system was employed to characterize uncertainty in weather forecasts. It was shown that there is relatively high uncertainty in contrails' aCCF due to the high variability among ensemble members of relative humidity. A heuristic algorithm was employed and implemented on graphics processing units to solve the proposed robust trajectory optimization in a computationally fast manner. The effectiveness of the proposed approach was explored in two scenarios. It was concluded that the best mitigation potential is obtained when the aircraft flies through contrails-sensitive areas for the cost optimal routing option. For a specific case of this scenario, a 55% reduction in climate impact was achieved at the expense of a 4.0% increase in cost. Due to relatively high uncertainty in the climate impact of contrails and their dominant climate effects, the net ATR was highly uncertain for the cases aircraft flew through PCFA. However, by moving toward trajectories with lower climate impacts (mainly achieved by avoiding the formation of persistent contrails), the dispersions of climate impacts were reduced. For the case with no formation of persistent contrails, the aircraft tended to reduce the climate impacts associated with other species at the expense of a relatively higher cost. However, 23% of climate impact could still be reduced by accepting a 3% increase in cost, and since no contrails were formed, the results were almost deterministic.

Code availability. The robust aircraft trajectory optimization technique presented in the paper is released as an open-source Python Library called ROOST V1.0 (Robust Optimization of Structured Trajectories).
It is developed at https://github.com/Abolfazl-Simorgh/roost, and is available via the DOI (https://doi.org/10.5281/zenodo.7121862). It is distributed under the GNU Lesser General Public Licence (Version 3.0). All the results presented in the paper were obtained using ROOST. To run the examples, one needs the BADA4.0 license. For the future release of the library, we aim to make the library compatible with open-source aircraft performance models such as OpenAP (Sun et al., 2020).

Data availability. The ERA5 data sets used in this study can be freely accessed from the respective repositories after registration. ERA5 data were retrieved from the Copernicus Climate Data Store (https://cds.climate.copernicus.eu/, European Reanalysis 5, 2020). Last access:05/2022.

https://doi.org/10.5194/egusphere-2022-1010
Preprint. Discussion started: 15 November 2022

Author contributions. Conceptualization, AS and MS; development of the library (ROOST V1.0), DG-A.; incorporation of climate impacts to the library, AS; algorithmic climate change functions, SD, SM, and FY; writing—original draft, AS and MS; writing—review and editing, AS, MS, DG-A, SM, VG, SD, SB, HY, FL, BL, MMM, FY, and FC; All authors have read and agreed to the published version of the manuscript.

Competing interests. The authors declare no conflict of interest.

Acknowledgements. This research was carried out as a part of the project EU project FlyATM4E. FlyATM4E has received funding from the SESAR Joint Undertaking under the European Union's Horizon 2020 research and innovation programme under grant agreement No 891317. The JU receives support from the European Union's Horizon 2020 research and innovation programme and the SESAR JU members other than the Union.

https://doi.org/10.5194/egusphere-2022-1010
Preprint. Discussion started: 15 November 2022

References

AMS-Council: Enhancing weather information with probability forecasts, Bull. Amer. Meteor. Soc, 89, 1049–1053, 2008.

Appleman, H.: The formation of exhaust condensation trails by jet aircraft, Bulletin of the American Meteorological Society, 34, 14–20, 1953.

Bauer, P., Thorpe, A., and Brunet, G.: The quiet revolution of numerical weather prediction, Nature, 525, 47–55, https://doi.org/10.1038/nature14956, 2015.

Bonami, P., Olivares, A., Soler, M., and Staffetti, E.: Multiphase mixed-integer optimal control approach to aircraft trajectory optimization, Journal of Guidance, Control, and Dynamics, 36, 1267–1277, 2013.

Campbell, S., Neogi, N., and Bragg, M.: An optimal strategy for persistent contrail avoidance, in: AIAA Guidance, Navigation and Control Conference and Exhibit, p. 6515, 2008.

Dietmüller, S., Matthes, S., Dahlmann, K., Yamashita, H., Simorgh, A., Soler, M., Linke, F., Lührs, B., Meuser, M. M., Weder, C., Grewe, V., Yin, F., and Castino, F.: A python library for computing individual and merged non-CO_2 algorithmic climate change functions: CLIMaCCF V1.0, Geoscientific Model Development Discussions, 2022, 1–33, https://doi.org/10.5194/gmd-2022-203, 2022.

DuBois, D. and Paynter, G. C.: "Fuel Flow Method2" for Estimating Aircraft Emissions, SAE Transactions, pp. 1–14, 2006.

Frömming, C., Grewe, V., Jöckel, P., Brinkop, S., Dietmüller, S., Garny, H., Ponater, M., Tsati, E., and Matthes, S.: Climate cost functions as a basis for climate optimized flight trajectories, Air Traffic Semin, 239, 1–9, 2013.

Gallo, E., Navarro, F., Nuic, A., and Iagaru, M.: Advanced Aircraft Performance Modeling for ATM: Bada 4.0 Results, in: 2006 ieee/aiaa 25TH Digital Avionics Systems Conference, pp. 1–12, IEEE, https://doi.org/10.1109/dasc.2006.313660, 2006.

Gierens, K. M., Lim, L., and Eleftheratos, K.: A review of various strategies for contrail avoidance, Open Atmospheric Science Journal, 2, 1–7, 2008.

González-Arribas, D., Soler, M., and Sanjurjo-Rivo, M.: Robust aircraft trajectory planning under wind uncertainty using optimal control, Journal of Guidance, Control, and Dynamics, 41, 673–688, 2018.

Gonzalez Arribas, D., Andres-Enderiz, E., Soler, M., Jardines, A., and Garcia-Heras, J.: Probabilistic 4D Flight Planning in Structured Airspaces through Parallelized Simulation on GPUs, in: International Conference on Research in Air Transportation (ICRAT), 2020.

Graver, B. and Rutherford, D.: Transatlantic airline fuel efficiency ranking, 2017, International Council on Clean Transportation, 2018.

Grewe, V. and Dahlmann, K.: How ambiguous are climate metrics? And are we prepared to assess and compare the climate impact of new air traffic technologies?, Atmospheric Environment, 106, 373–374, 2015.

Grewe, V., Champougny, T., Matthes, S., Frömming, C., Brinkop, S., Søvde, O. A., Irvine, E. A., and Halscheidt, L.: Reduction of the air traffic's contribution to climate change: A REACT4C case study, Atmospheric Environment, 94, 616–625, 2014a.

Grewe, V., Frömming, C., Matthes, S., Brinkop, S., Ponater, M., Dietmüller, S., Jöckel, P., Garny, H., Tsati, E., Dahlmann, K., et al.: Aircraft routing with minimal climate impact: The REACT4C climate cost function modelling approach (V1. 0), Geoscientific Model Development, 7, 175–201, 2014b.

Grewe, V., Rao, A. G., Grönstedt, T., Xisto, C., Linke, F., Melkert, J., Middel, J., Ohlenforst, B., Blakey, S., Christie, S., et al.: Evaluating the climate impact of aviation emission scenarios towards the Paris agreement including COVID-19 effects, Nature Communications, 12, 1–10, 2021.

Guide, D.: Cuda c programming guide, NVIDIA, July, 29, 31, 2013.

https://doi.org/10.5194/egusphere-2022-1010
Preprint. Discussion started: 15 November 2022

Hartjes, S., Hendriks, T., and Visser, D.: Contrail mitigation through 3D aircraft trajectory optimization, in: 16th AIAA Aviation Technology, Integration, and Operations Conference, p. 3908, 2016.

Jelinek, F.: The Advanced Emission Model (AEM3)-Validation Report, Ratio, 306, 1–13, 2004.

Klöckner, A., Pinto, N., Lee, Y., Catanzaro, B., Ivanov, P., and Fasih, A.: PyCUDA and PyOpenCL: A scripting-based approach to GPU run-time code generation, Parallel Computing, 38, 157–174, 2012.

Lee, D. S., Fahey, D., Skowron, A., Allen, M., Burkhardt, U., Chen, Q., Doherty, S., Freeman, S., Forster, P., Fuglestvedt, J., et al.: The contribution of global aviation to anthropogenic climate forcing for 2000 to 2018, Atmospheric Environment, 244, 117 834, 2021.

Lim, Y., Gardi, A., and Sabatini, R.: Optimal aircraft trajectories to minimize the radiative impact of contrails and CO_2, Energy Procedia, 110, 446–452, 2017.

Lührs, B., Niklass, M., Froemming, C., Grewe, V., and Gollnick, V.: Cost-benefit assessment of 2D and 3D climate and weather optimized trajectories, in: 16th AIAA Aviation Technology, Integration, and Operations Conference, p. 3758, 2016.

Lührs, B., Linke, F., Matthes, S., Grewe, V., and Yin, F.: Climate impact mitigation potential of European air traffic in a weather situation with strong contrail formation, Aerospace, 8, 50, 2021.

Mania, H., Guy, A., and Recht, B.: Simple random search of static linear policies is competitive for reinforcement learning, in: Advances in Neural Information Processing Systems, pp. 1800–1809, 2018.

Matthes, S., Schumann, U., Grewe, V., Frömming, C., Dahlmann, K., Koch, A., and Mannstein, H.: Climate optimized air transport, in: Atmospheric physics, pp. 727–746, Springer, 2012.

Matthes, S., Grewe, V., Dahlmann, K., Frömming, C., Irvine, E., Lim, L., Linke, F., Lührs, B., Owen, B., Shine, K., et al.: A concept for multi-criteria environmental assessment of aircraft trajectories, Aerospace, 4, 42, 2017.

Matthes, S., Lührs, B., Dahlmann, K., Grewe, V., Linke, F., Yin, F., Klingaman, E., and Shine, K. P.: Climate-optimized trajectories and robust mitigation potential: Flying ATM4E, Aerospace, 7, 156, 2020.

Matthes, S., Dahlmann, K., Dietmüller, S., Baumann, S., Grewe, V., Yamashita, H., Soler, M., Simorgh, A., Linke, F., Lührs, B., M. Meuser, M., Weder, C., Castino, F., and Yin, F.: Concept for identifying robust eco-efficient aircraft trajectories: Methodological concept of climate-optimised aircraft trajectories in FlyATM4E, Applied Sciences (In preparation), 2022.

Niklaß, M., Gollnick, V., Lührs, B., Dahlmann, K., Froemming, C., Grewe, V., and van Manen, J.: Cost-benefit assessment of climate-restricted airspaces as an interim climate mitigation option, Journal of Air Transportation, 25, 27–38, 2017.

Niklaß, M., Lührs, B., Grewe, V., Dahlmann, K., Luchkova, T., Linke, F., and Gollnick, V.: Potential to reduce the climate impact of aviation by climate restricted airspaces, Transport Policy, 83, 102–110, 2019.

Niklaß, M., Grewe, V., Gollnick, V., and Dahlmann, K.: Concept of climate-charged airspaces: a potential policy instrument for internalizing aviation's climate impact of non-CO_2 effects, Climate Policy, 21, 1066–1085, 2021.

Penner, J. E., Lister, D., Griggs, D. J., Dokken, D. J., and McFarland, M.: Aviation and the global atmosphere: a special report of the Intergovernmental Panel on Climate Change, 1999.

Scherer, C.: Global Market Forecast Cities, Airports & Aircraft 2019-2038, AIRBUS SAS, 31707, 2019.

Schmidt, E.: Die entstehung von eisnebel aus den auspuffgasen von flugmotoren, Schriften der Deutschen Akademie der Luftfahrtforschung, Verlag R. Oldenbourg, München, Heft 44, 5, 1–15, 1941.

Simorgh, A., Soler, M., González-Arribas, D., Matthes, S., Grewe, V., Dietmüller, S., Baumann, S., Yamashita, H., Yin, F., Castino, F., et al.: A Comprehensive Survey on Climate Optimal Aircraft Trajectory Planning, Aerospace, 9, 146, 2022.

https://doi.org/10.5194/egusphere-2022-1010
Preprint. Discussion started: 15 November 2022

Soler, M., Zou, B., and Hansen, M.: Flight trajectory design in the presence of contrails: Application of a multiphase mixed-integer optimal control approach, Transportation Research Part C: Emerging Technologies, 48, 172–194, 2014.

Sridhar, B., Ng, H. K., and Chen, N. Y.: Aircraft trajectory optimization and contrails avoidance in the presence of winds, Journal of Guidance, Control, and Dynamics, 34, 1577–1584, 2011.

Sun, J., Hoekstra, J. M., and Ellerbroek, J.: OpenAP: An open-source aircraft performance model for air transportation studies and simulations, Aerospace, 7, 104, 2020.

van Manen, J. and Grewe, V.: Algorithmic climate change functions for the use in eco-efficient flight planning, Transportation Research Part D: Transport and Environment, 67, 388–405, 2019.

Vitali, A., Battipede, M., and Lerro, A.: Multi-Objective and Multi-Phase 4D Trajectory Optimization for Climate Mitigation-Oriented Flight Planning, Aerospace, 8, 395, 2021.

WMO: Guidelines on ensemble prediction systems and forecasting, World Meteorological Organization Weather Climate and Water, 1091, 2012.

Yamashita, H., Yin, F., Grewe, V., Jöckel, P., Matthes, S., Kern, B., Dahlmann, K., and Frömming, C.: Newly developed aircraft routing options for air traffic simulation in the chemistry–climate model EMAC 2.53: AirTraf 2.0, Geoscientific Model Development, 13, 4869–4890, 2020.

Yamashita, H., Yin, F., Grewe, V., Jöckel, P., Matthes, S., Kern, B., Dahlmann, K., and Frömming, C.: Analysis of aircraft routing strategies for north atlantic flights by using AirTraf 2.0, Aerospace, 8, 33, 2021.

Yin, F., Grewe, V., Frömming, C., and Yamashita, H.: Impact on flight trajectory characteristics when avoiding the formation of persistent contrails for transatlantic flights, Transportation Research Part D: Transport and Environment, 65, 466–484, 2018a.

Yin, F., Grewe, V., van Manen, J., Matthes, S., Yamashita, H., Linke, F., and Lührs, B.: Verification of the ozone algorithmic climate change functions for predicting the short-term NO_x effects from aviation en-route, in: International Conference on Research in Air Transportation (ICRAT), 2018b.

Yin, F., Grewe, V., Castino, F., Rao, P., Matthes, S., Dahlmann, K., Dietmüller, S., Frömming, C., Yamashita, H., Peter, P., Klingaman, E., Shine, K., Lührs, B., and Linke, F.: Predicting the climate impact of aviation for en-route emissions: The algorithmic climate change function submodel ACCF 1.0 of EMAC 2.53, Geoscientific Model Development Discussions, 2022, 1–34, https://doi.org/10.5194/gmd-2022-220, 2022.